1967

Stress Distribution in and Deflection Properties of Tri-plate Beams in the Plastic Range

Richard Clarkson Cline

STRESS DISTRIBUTION IN AND DEFLECTION PROPERTIES OF TRI-PLATE BEAMS IN THE PLASTIC RANGE

BY

RICHARD CLARKSON CLINE

A thesis submitted
in partial fulfillment of the requirements for the
degree Master of Science, Major in Civil
Engineering, South Dakota
State University

1967

STRESS DISTRIBUTION IN AND DEFLECTION PROPERTIES OF TRI-PLATE BEAMS IN THE PLASTIC RANGE

This thesis is approved as a creditable and independent investigation by a candidate for the degree, Master of Science, and is acceptable as meeting the thesis requirements for this degree, but without implying that the conclusions reached by the candidate are necessarily the conclusions of the major department.

Thesis Adviser Date

Head, Civil Engineering Department Date

ACKNOWLEDGMENT

The author wishes to express his gratitude to Dr. Zaher Shoukry, Associate Professor, Department of Civil Engineering, for his wise counsel and encouragement throughout the course of this project. Dr. Shoukry's valued assistance and inspiring help is sincerely appreciated. To him, the author is truly indebted.

This thesis is dedicated to the author's wife, Diane, whose loyal encouragement and sacrifice has made this project possible.

RCC

TABLE OF CONTENTS

Chapter Page

LIST OF FIGURES

Figure Page

LIST OF TABLES

CHAPTER I

INTRODUCTION

General

Tri-plate beams combine versatility, economy, and strength in steel design. These beams have many applications which indicate increased efficiency and economy in long-span plate girder construction. Their structural advantages are almost unlimited.

Tri-plate beams are fabricated by welding three different types of steel to form an I-section. Each flange and the web of the section is fabricated out of a different yield strength steel. Because the flanges of a beam contribute most of its moment resistance, the use of high-strength steel in the flanges is desirable. However, in tri-plate beams, the tension flange consists of a higher strength steel than does the compression flange because of the buckling liability of the compression flange. The utilization of a higher strength steel in the tension flange also makes possible a reduction in the tension flange cross sectional area. Because of its low moment carrying capacity, the web is fabricated out of a lower strength steel.

The idea of tri-plate beams is not totally new, having previously been used to a very limited extent in plate girder construction. However, these beams have not previously been recognized and analyzed as an independent part of the girder system. In a way, the tri-plate concept is analogous to composite design, where the reinforced concrete slab is used as a large compression flange, the web is of a low strength steel, and the tension flange is composed of a high-strength steel.

High-strength steel beams have indicated increased economy in steel design. Tri-plate beams will offer still more economy while, at the same time, provide new possibilities in construction with structural steel. Furthermore, these beams represent savings in material and the availability of lighter sections that can meet the competition presented by prestressed concrete.

Background

The rapid increase in the use of prestressed concrete construction has resulted in a search for more efficient and economical methods of construction with structural steel by the steel industry. Starting about thirty years ago, the steel industry has conducted a continuing program of research to develop steels of lower cost and higher performance. As a direct result, a large selection of new economic and high performance steel is now available to the designer.

The 1963 AISC (American Institute of Steel Construction) specification allows the use of a variety of high-strength and high-strength low-alloy steels such as the present ASTM-A36, A440, A441, and A242 designations. The yield strength of these new steels may vary from 36,000 psi for A36 carbon steel to 50,000 psi for A441 high-strength low-alloy steel. At present, however, the steel industry is promoting a new group of higher strength structural steels that offer possible weight and cost savings over the steels currently covered by the AISC specification. These new heat-treated constructional alloy steels have a yield strength in the vicinity of 100,000 psi.

With these new steels at its disposal, the steel industry began searching for a structural member that could favorably compete with the economy and efficiency of prestressed concrete. With their high yield strength, good ductility, and excellent welding qualities, these newly developed high-strength steels indicate that they can offer the desired competitive design.

The structural steels that are widely used at present can be divided into the following three broad categories:

1. Structural carbon steels.
2. High-strength low-alloy steels.
3. Constructional alloy steels.

Pertinent information concerning the steels that are representative of these three categories is given in Table I.

Of particular significance in this study are the ASTM-A36, ASTM-A441, and "T-1" designations. A36 is a structural carbon steel. A441 is a low-alloy, mangenese-copper-vanadium steel intended for applications requiring cold forming, welding, and improved toughness properties. USS "T-1" constructional alloy steels are heat-treated steels suitable for welded structures.

In contrast with many of the higher strength steels available in the past, the modern high-strength steels show more favorable price-to-strength ratios than structural carbon steel.[1]

---

[1] G. Haaijer, "Economy of High Strength Steel Structural Members," Transactions, American Society of Civil Engineers, vol. 128, 1963, p. 820.

Table I

Mechanical Properties of Constructional Steels

Category	Steel	Thickness Range (inches)	Yield Point (psi)	Tensile Strength (psi)
Structural Carbon Steel	ASTM-A7 ASTM-A36	All thicknesses 4 and under	33,000 36,000	60,000 to 75,000
High-Strength Steel	ASTM-A440	3/4 and under over 3/4 to 1 1/2 incl. over 1 1/2 to 4 incl.	50,000 46,000 42,000	70,000 min. 67,000 min. 63,000 min.
	ASTM-A441	3/4 and under over 3/4 to 1 1/2 incl. over 1 1/2 to 4 incl.	50,000 46,000 42,000	70,000 min. 67,000 min. 63,000 min.
	USS COR-TEN	1/2 and under over 1/2 to 1 1/2 incl. over 1 1/2 to 3 incl.	50,000 47,000 43,000	70,000 min. 67,000 min. 63,000 min.
Constructional Alloy Steel	USS "T-1"	3/16 to 2 1/2 incl. over 2 1/2 to 4 incl.	100,000 90,000	115,000 to 135,000 105,000 to 135,000

That is, high-strength steels show a relative increase in price that is less than the relative increase in yield strength. As a result, the application of higher strength steels to structures in which the higher strength can be utilized often results in significant material-cost savings.

Since the moment resistance provided by a beam or girder is contributed mostly by the flanges, replacing the flanges with higher strength steel results in considerable saving in cost as well as in weight. Cost and weight analyses have indicated that beams constructed with high-strength steel flanges have resulted in as much as 20 percent saving in cost and as much as 40 percent reduction in weight. Since the web of a plate girder accounts for a large portion of its weight but contributes only a small part of its moment carrying capacity, the use of cheaper low-strength steel for the web would be desirable.

The proper selection of material is one of the essential steps in a design to ensure that the structure will meet its functional requirements with adequate safety and minimum cost. The question of economics includes the base price of the material, fabrication costs, freight, effect of dead weight of the structure on foundation costs, optimum space utilization, and some other factors. With these considerations in mind, the tri-plate beam will be a significant contribution in the area of steel construction.

Review of Past Investigations

Although the use of girders with carbon steel webs and higher strength flanges of structural silicon steel dates back many years, the

theoretical behavior of such members has not been analyzed extensively, and little experimental work has been performed to verify the theoretical behavior.

The availability of the new high-strength structural steels has prompted the recent investigations of the behavior of hybrid beams that are built up by welding higher strength steel flanges to lower strength steel webs. The results of studies presented by Haaijer in 1961[2] indicate that through the optimum design of structural members, the application of high-strength steels can lead to lighter weight structures and often to significant material-cost savings.

Tests conducted in 1961 by A. A. Toprac at the University of Texas yielded the following conclusions:[3]

1. When a girder with high-strength steel flanges and carbon steel web is loaded so that the yield point of the web is exceeded, a redistribution of stress will occur and allow the girder to continue to deform elastically. When, after having the load removed, the girder is reloaded, complete elastic behavior extends over a load range almost twice the first range.

---

[2] Ibid.

[3] A. A. Toprac and R. A. Engler, "Plate Girders With High Strength Steel Flanges and Carbon Steel Webs," Proceedings, American Institute of Steel Construction, 1961, p. 91.

2. Girders of this type are particularly adaptable to long spans where the ratio of dead-to total load is high and live load deflection is not critical.
3. The fact that the web is stressed beyond its yield strength has little adverse effect on the ultimate carrying capacity of the member.

More recent theoretical and experimental investigations of the behavior of hybrid beams have provided new and valuable information concerning the design of such beams. As a result of investigations made in 1964, Frost and Schilling[4] have concluded that because the reduction in bending strength caused by shear in hybrid beams is small, it is satisfactory to design hybrid beams independently for bending and shear. In 1966, tests conducted by Sarsam[5] showed that thin webs can be used satisfactorily in hybrid beams, especially for laterally supported, long spans. Also pointed out was the fact that the stability rather than the stresses will control the design for thin web hybrid beams because of the critical lateral and torsional buckling of the compression flange.

---

[4] R. W. Frost and C. G. Schilling, "Behavior of Hybrid Beams Subjected to Static Loads," Journal of the Structural Division, ASCE, vol. 90, no. ST3, Proc. Paper 3928, 1964, p. 86.

[5] Jamal B. Sarsam, "Behavior of Thin Web Hybrid Beams Subjected to Static Loads," thesis presented to South Dakota State University, Brookings, South Dakota, in August, 1965, in partial fulfillment of the requirements for the degree of Master of Science, p. 63.

The need for further testing of beams fabricated from high-strength steel is evident. The study of tri-plate beams can furnish additional insight into the behavior of such sections and provide for new innovations in structural steel design.

Object and Scope of Investigation

The selection of A441 high-strength low-alloy steel for the compression flanges and A36 carbon steel for the webs was made because of the increasing demand and popularity of these two types of steel. In 1963, with its favorable price-to-strength ratio and excellent weldability, A441 steel was used in 87 percent of the buildings fabricated from high-strength steel.

In this investigation, "T-1" constructional alloy steel has been used for the tension flanges. Although it is not yet covered by the AISC specification, it has nevertheless been chosen because of its high-strength properties. This use of "T-1" steel will also provide additional information about its structural behavior, weldability, and adaptability for future building construction.

The objectives of the investigation reported herein are as follows:

1. To investigate the structural behavior of tri-plate beams, both in the elastic and plastic range.
2. To study the stress distribution in the webs and flanges of tri-plate beams.
3. To determine their strength and mode of failure.

4. To present a simplified method of stress and deflection analysis and compare calculated values to observed strengths and deflections.

5. To investigate the fatigue properties of tri-plate beams.

This study has been limited to pure bending and to combined shear and bending. These two cases are illustrated in Figure 1. Zone A is pure bending; Zones B and C are combined shear and bending. The plastic design method of analysis has been used in the theoretical considerations to obtain the practical upper limit of strength of the beams.

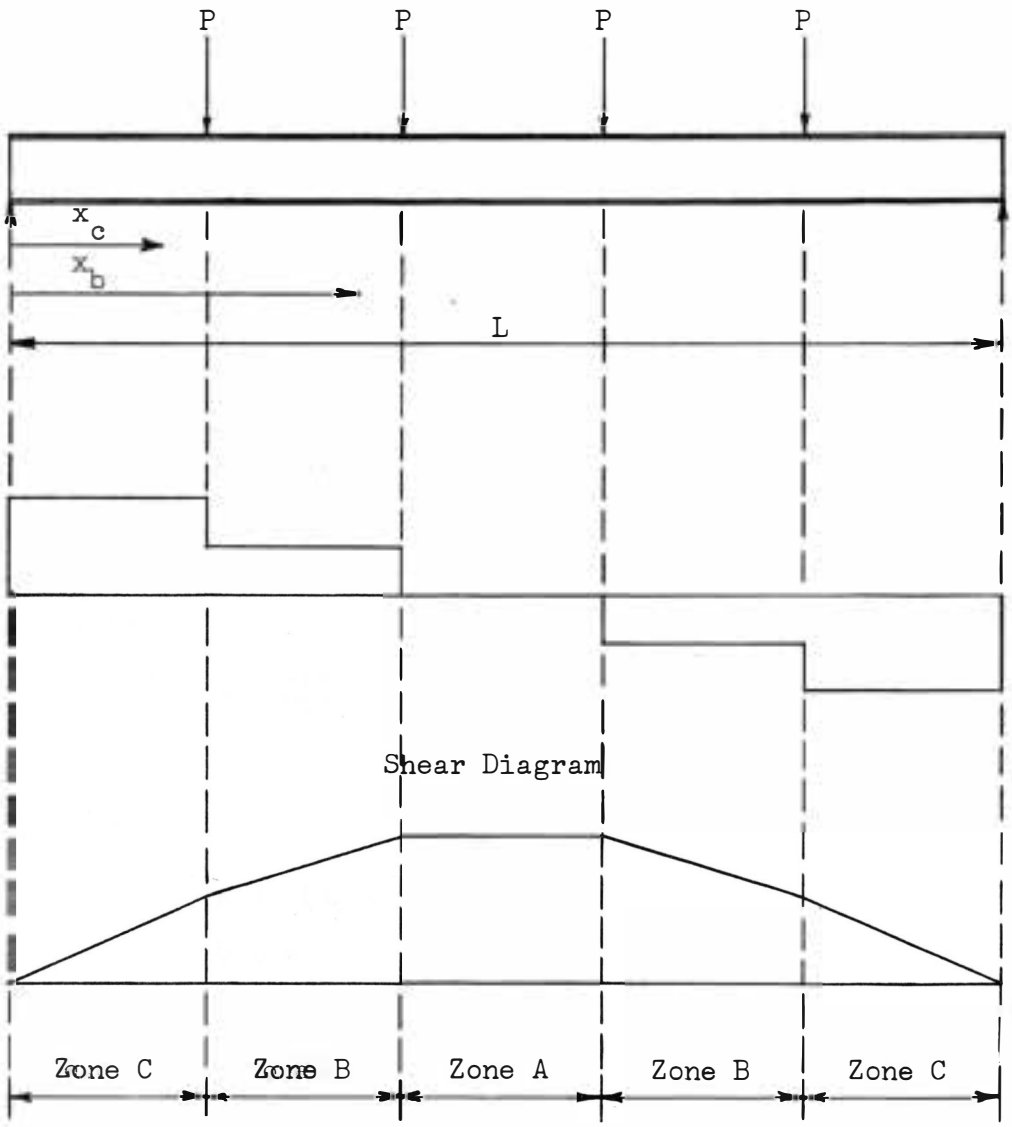

Figure 1. Typical Shear-Moment Diagrams for Test Specimens

CHAPTER II

THEORETICAL BEHAVIOR OF TRI-PLATE BEAMS

Introduction

The behavior of tri-plate beams in pure bending and combined shear and bending will be investigated under static loads. The load-deflection or moment-curvature relationship, and the progressive stages of yielding from the initial yield to the fully plastic condition will be specifically analyzed and compared with hybrid beams.

Figure 1 shows the shear and moment distribution resulting from the loads P on the test specimens. The values for the shear and moment at the different zones along the beam are expressed as follows:

Zone A:

$$M = \frac{3PL}{5}$$

$$V = 0$$

Zone B:

$$M = P(x_b + \frac{L}{5})$$

$$V = P$$

Zone C:

$$M = 2Px_c$$

$$V = 2P$$

where

P = the concentrated load

L = the length of span

x_b, x_c = the distance from the support to any point in the corresponding zone

In the subsequent analysis, the following assumptions are used:

1. The stress-strain relationship for all parts of a tri-plate beam can be idealized to consist of the two straight lines shown in Figure 2. The equations of these two lines are

$$\sigma = E\epsilon \quad \text{(elastic range)}$$

$$\sigma = \sigma_y \quad \text{(plastic range)}$$

where

σ = the stress at the extreme fibers of the section

σ_y = the yield stress at the extreme fibers of the section

E = the modulus of elasticity of steel

ϵ = the elastic strain

2. Deformations are sufficiently small so that tan (tangent) ϕ can be considered equal to ϕ except for large values of ϕ that occur in the fully plastic range. (ϕ is the curvature)

Pure Bending

The analysis of a tri-plate beam can best be explained by means of a bending moment versus curvature diagram as that shown in Figure 3. As the moment increases, the moment-curvature curve progresses through six stages of yielding. Within Stage I and up to the yield moment of the bottom web fibers, M_{y_1}, the stress distribution is linear and varies according to the flexural formula:

$$\sigma = \frac{My}{I}$$

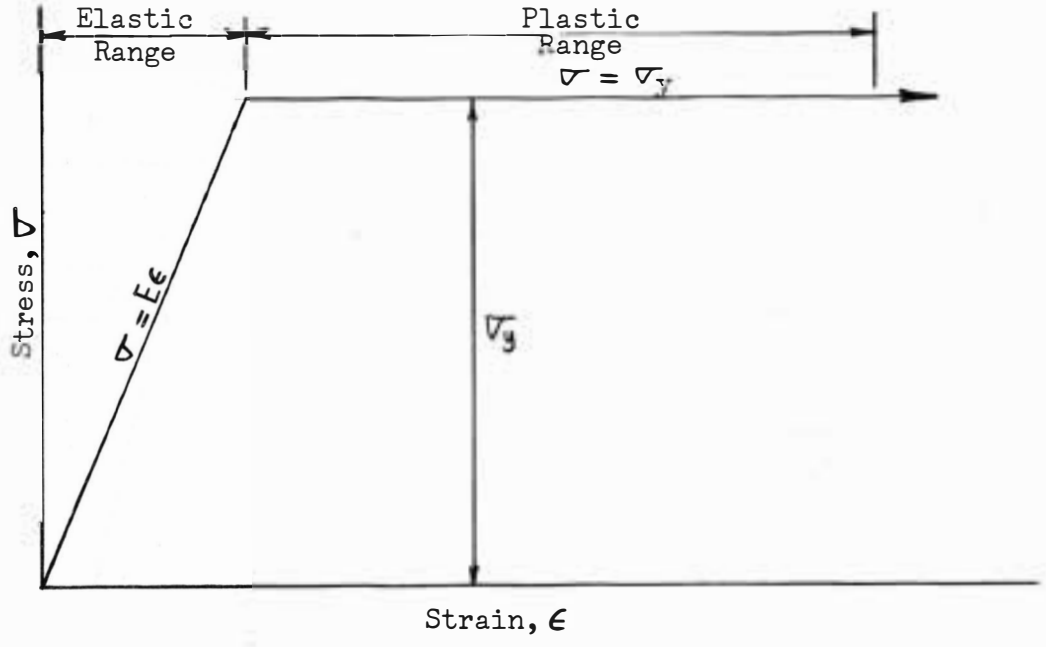

Figure 2. Idealized Stress-Strain Diagram

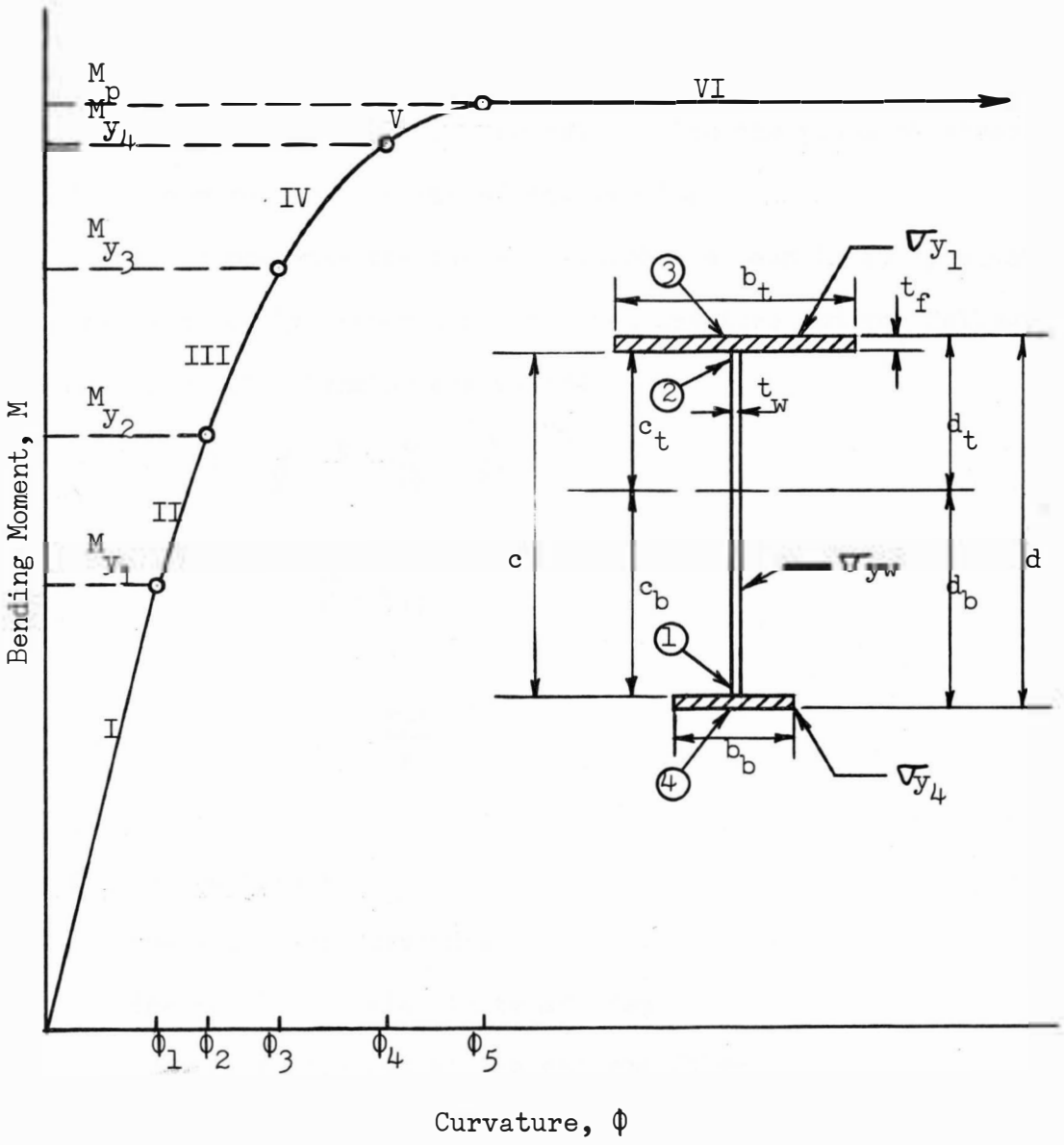

Figure 3. Moment-Curvature Relationship for a Tri-Plate Beam

where

σ = the stress at the plane under consideration

M = the resisting moment of the section

y = the distance from the neutral axis to the plane of stresses

I = the moment of inertia of the section

Stage I represents the range in which the beam is fully elastic. The moment is directly proportional to the curvature and the following relations for elastic bending are valid:

$$\phi = \frac{1}{\rho} = \frac{\epsilon}{y} = \frac{\sigma}{Ey} = \frac{M}{EI} \tag{1}$$

From which

$$M = EI\phi \tag{2}$$

and

$$M_y = \frac{\sigma_y I}{y} \tag{3}$$

where

ϕ = the curvature

ρ = the radius of curvature

E = the modulus of elasticity of steel

σ_y = the yield stresses at the extreme fibers

The initial yielding of the tri-plate beam takes place only in the bottom fibers of the web. Since the extreme bottom fibers of the web are at a distance c_b from the neutral axis, formula (3) becomes

$$M_{y_1} = \frac{\sigma_{yw} I}{c_b} \tag{4}$$

where

M_{y_1} = the lower web yield moment

σ_{yw} = the yield stress of the web

c_b = the distance from the neutral axis to the extreme bottom web fibers

As the moment increases beyond the upper limit of Stage I, the M-ϕ curve passes through five other stages. Figure 4 shows the development of strain, stress, and yield distribution as the tri-plate beam is bent in successive stages beyond the elastic limit (Stage I) and up to the plastic limit (Stage VI).

Stage II represents the range in which yielding develops in the extreme bottom fibers of the web, while the extreme top web fibers and the flanges remain elastic, as shown in Figure 4. In this stage as well as in Stage I, the strain varies linearly through the depth of the cross section; however, in Stage II, the stress is no longer directly proportional to the strain and the stress distribution is as shown in Figure 4. The moment at any given stage can be obtained by integrating the stress areas according to the general expression

$$M = \int_{Area} \sigma dAy$$

Thus for Stage II, the moment corresponding to a given curvature can be obtained by integrating the first moment of the stress over the entire beam cross section, which gives

$$M = E\phi(I_{ft} + I_{fb}) + \sigma_{yw}\frac{t_w c_b^2}{2} + \frac{t_w \sigma_{yw}^3}{6E^2\phi^2} \qquad (5)$$

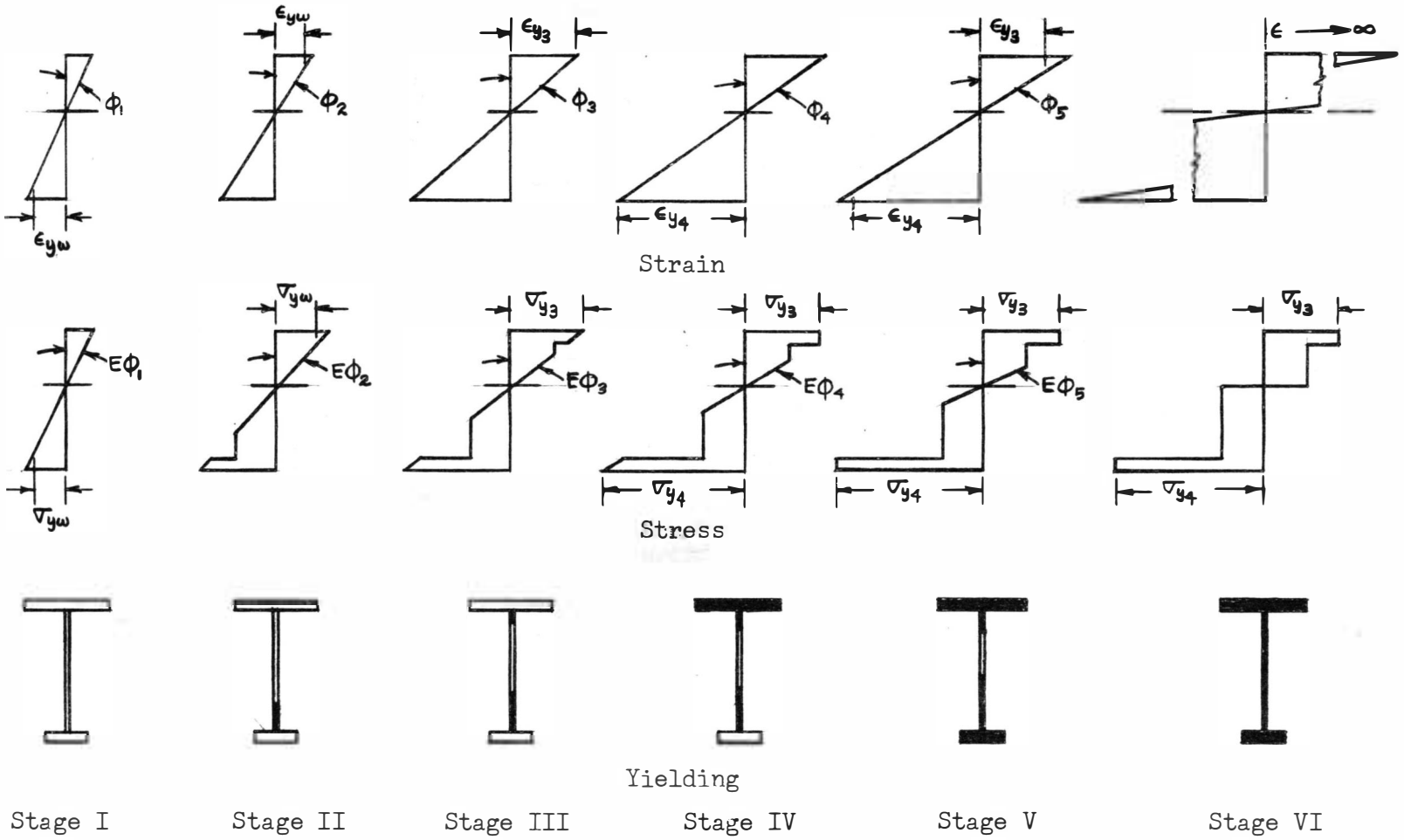

Figure 4. Distribution of Strain, Stress, and Yielding at the Upper Limit of Each Stage of Loading

where

I_{ft} = the moment of inertia of the top flange about the neutral axis

I_{fb} = the moment of inertia of the bottom flange about the neutral axis

t_w = the web thickness

The integration details of the derivation are given in Appendix A. Considering that the maximum elastic strain for Stage II is given by

$$\epsilon = \frac{\sigma_{yw}}{E}$$

and

$$\tan \phi = \phi = \frac{\epsilon}{c_t}$$

Then

$$E\phi = \frac{\sigma_{yw}}{c_t} \tag{6}$$

where

c_t = the distance from the neutral axis to the extreme top web fibers

By replacing $E\phi$ in equation (5) with $\frac{\sigma_{yw}}{c_t}$, the value of the moment at the upper limit of Stage II is given by

$$M_{y_2} = \sigma_{yw}\left(\frac{I_{ft} + I_{fb}}{c_t}\right) + \sigma_{yw}\left(\frac{t_w c_b^2}{2} + \frac{t_w c_t^2}{6}\right) \tag{7}$$

In Stage III yielding develops in the extreme top web fibers while the flanges are still elastic. By integrating the stress areas, the moment corresponding to a given curvature is

$$M = E\phi\left(I_{ft} + I_{fb}\right) + \sigma_{yw} Z_w - \frac{t_w \sigma_{yw}^3}{3E^2\phi^2} \tag{8}$$

where

Z_w = the plastic modulus of the web

The upper limit of this stage is the moment that initiates yielding in the upper flange; the strain is then related to the curvature by

$$\epsilon = \frac{\sigma_{y_3}}{E}$$

and $$\tan \phi = \phi = \frac{\epsilon}{d_t}$$

From which

$$E\phi = \frac{\sigma_{y_3}}{d_t} \tag{9}$$

where

σ_{y_3} = the yield stress of the upper flange

d_t = the distance from the neutral axis to the extreme top flange fibers

Since equation (9) is the curvature relationship at the upper limit of Stage III, equation (8) becomes

$$M_{y_3} = \sigma_{y_3}\left(\frac{I_{ft} + I_{fb}}{d_t}\right) + \sigma_{yw} Z_w - \frac{t_w d_t^2}{3}\frac{\sigma_{yw}^3}{\sigma_{y_3}^2} \tag{10}$$

In Stages IV, V, and VI the behavior of the beam is similar to that in Stages II and III, and the moment corresponding to a given curvature can be obtained from the stress distribution for that curvature. Stage IV represents the range in which yielding progresses through the upper flange. The M-ϕ relationship for this stage is

$$M = \sigma_{y_3} Z_{ft} + E\phi I_{fb} + \sigma_{yw} Z_w - \frac{t_w \sigma_{yw}^3}{3E^2\phi^2} \tag{11}$$

where

Z_{ft} = the plastic modulus of the top flange

The curvature relationship at the upper limit of this stage (initial yielding of the lower flange) is given by

$$E\phi = \frac{\sigma_{y_4}}{d_b} \tag{12}$$

Then equation (11) becomes

$$M_{y_4} = \sigma_{y_3} Z_{ft} + \frac{\sigma_{y_4} I_{fb}}{d_b} + \sigma_{yw} Z_w - \frac{t_w d_b^2}{3} \frac{\sigma_{yw}^3}{\sigma_{y_4}^2} \tag{13}$$

Stage V represents the range in which yielding progresses through the lower flange. In this stage, as in the other stages, the strain varies linearly through the depth of the cross section, however, in Stage V the strain exceeds the elastic strain of both flanges. In this stage most of the beam is in the plastic condition except a small portion around the neutral axis, as shown in Figure 4.

In Stage VI the remaining elastic portion of the web at the neutral axis becomes plastic, and the entire section is in the plastic condition. In the plastic range the moment-curvature relationship and the magnitude of the maximum plastic moment are similarly derived by considering the deformed structure and obtaining the corresponding curvature and moment. The M-ϕ relationship for Stage VI is determined as

$$M = \sigma_{yw} Z_w + \sigma_{y_3} Z_{ft} + \sigma_{y_4} Z_{fb} - \frac{t_w \sigma_{yw}^3}{3E^2\phi^2} \tag{14}$$

where

Z_{fb} = the plastic modulus of the bottom flange

Frost and Schilling recommend[6] that ϕ in equation (14) should be replaced by tan ϕ so that as ϕ approaches $\pi/2$, the moment approaches the fully plastic moment, M_p. Considering that the tan $\pi/2$ is undefined, equation (14) becomes

$$M_p = \sigma_{yw} Z_w + \sigma_{y_3} Z_{ft} + \sigma_{y_4} Z_{fb} \tag{15}$$

It can be seen from equation (15) that the expression for the plastic moment, M_p, is merely an application of the general plastic moment equation

$$M_p = \sigma_y Z$$

to each part of the beam. By multiplying the plastic modulus of each part of the beam by its respective yield stress, the plastic moment is obtained.

$$M_p = \sigma_{yw} \frac{t_w}{2} \left(c_t^2 + c_b^2\right) + \sigma_{y_3} b_t t_f \left(c_t + \frac{t_f}{2}\right) + \sigma_{y_4} b_b t_f \left(c_b + \frac{t_f}{2}\right) \tag{16}$$

where

$\frac{t_w}{2}\left(c_t^2 + c_b^2\right)$ = the plastic modulus of the web

$b_t t_f \left(c_t + \frac{t_f}{2}\right)$ = the plastic modulus of the upper flange

$b_b t_f \left(c_b + \frac{t_f}{2}\right)$ = the plastic modulus of the lower flange

The typical moment-curvature relationship of a hybrid beam indicates that, as the moment increases, the M-ϕ curve passes through four stages of yielding, as shown in Figure 5. The distribution of strain,

---

[6] Frost and Schilling, p. 60.

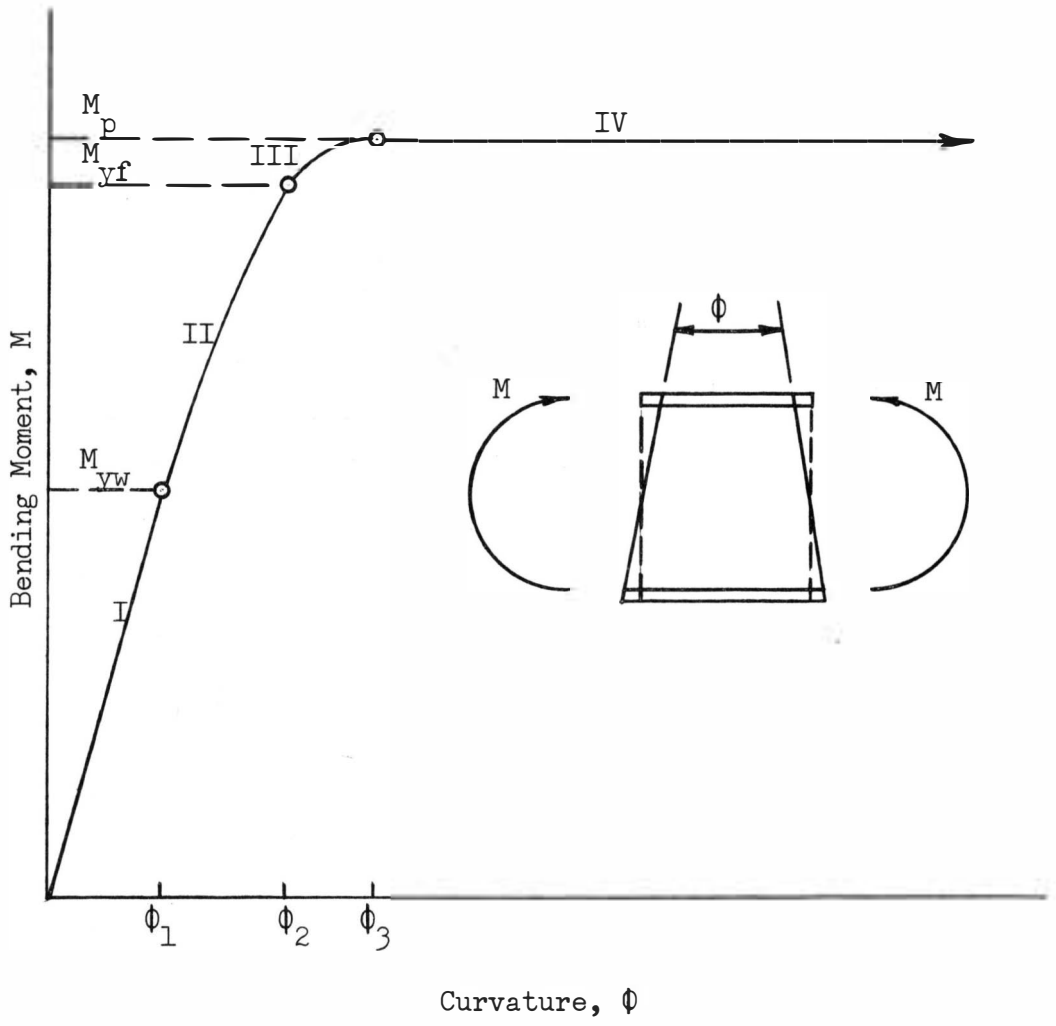

Figure 5. Moment-Curvature Relationship for a Hybrid Beam

stress, and yielding at the upper limit of each of these stages is shown in Figure 6. Whereas the extreme top and bottom fibers of the web of the hybrid beam begin yielding simultaneously at the upper limit of Stage I, the initial yielding of the tri-plate beam takes place only in the bottom fibers of the web. Also, the initial yielding in the web of a tri-plate beam begins at a lower moment value than it does in a hybrid beam.

Combined Shear and Bending

The effect of shear force on a tri-plate beam may limit the load to a value that is less than that which corresponds to the full plastic moment. This effect is especially true in the case of a short beam centrally loaded or a long beam with a concentrated load near the end.

In order to arrive at a basis for assuring that the full plastic moment will be reached, two possibilities must be considered:

1. General yielding of the web because of shear may occur in the presence of high moment-to-shear ratios.
2. After the beam has become partially plastic at a critical section because of flexural yielding, the intensity of shear stress at the centerline may reach the yield condition.

In cases of high moment-to-shear ratios (Case I), it can be assumed that the entire moment is taken by the flanges and that the shear is resisted by the web.

$$\tau = \frac{V}{A_w} \tag{17}$$

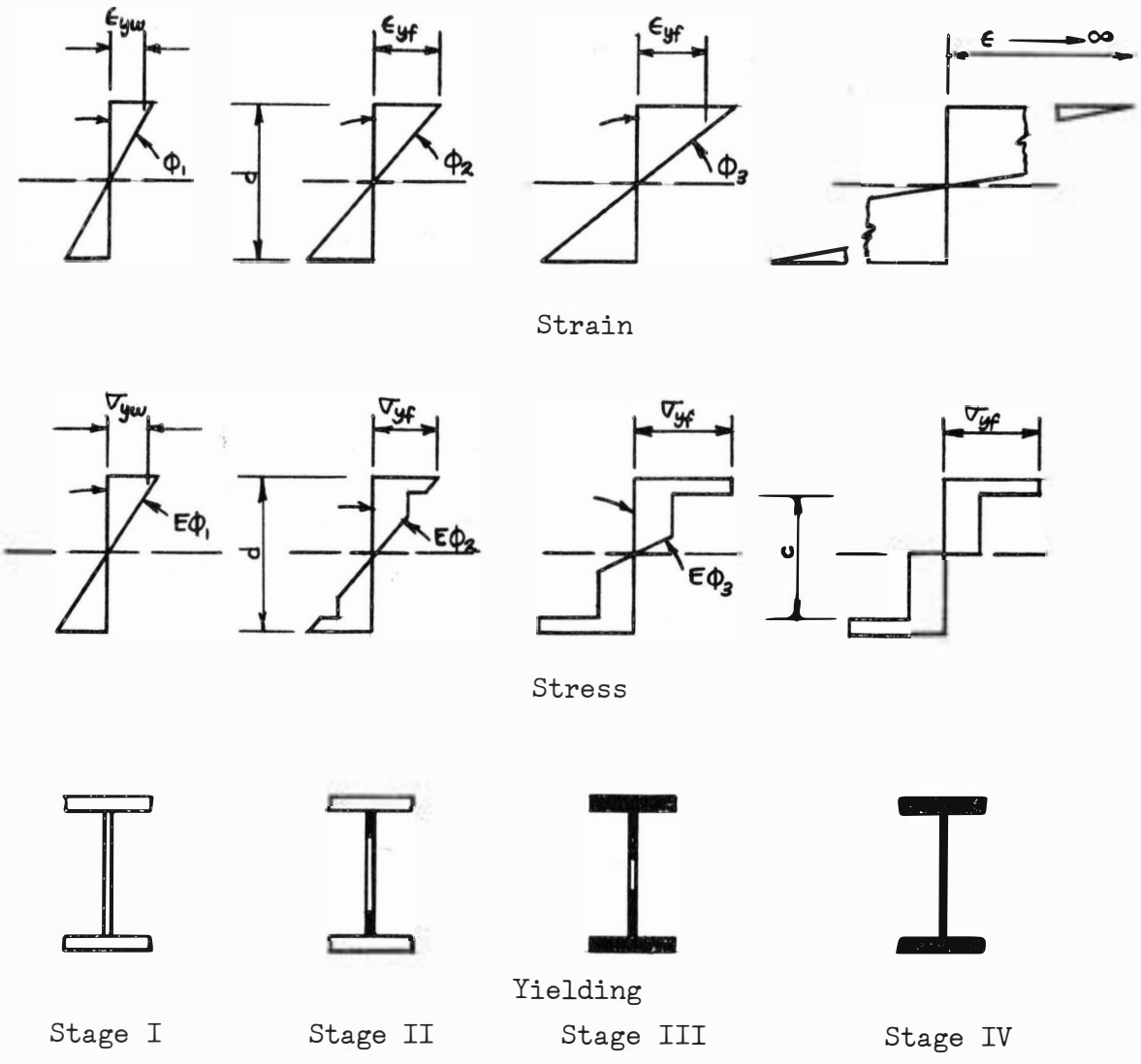

Figure 6. Distribution of Strain, Stress, and Yielding at the Upper Limit of Each Stage of Loading Hybrid Beam

where

τ = the shear stress in the web

V = the applied shear force

A_w = the cross sectional area of the web

From equation (17), the maximum possible shear according to this criterion is given by

$$V_{max} = V_p = \tau_y t_w c$$

where

V_p = the shear force that causes the web to become fully plastic

τ_y = the shear yield stress of the web

t_w = the thickness of the web

c = the depth of the beam

Using the Von Mises-Hencky[7] yield criterion for yielding under pure shear,

$$\tau_y = \frac{\sigma_{yw}}{\sqrt{3}} \tag{18}$$

the plastic shear force is given by

$$V_p = \frac{\sigma_{yw}}{\sqrt{3}} t_w c \tag{19}$$

Because that part of the web that yields in moment does not contribute to shear resistance, the shear stresses must be carried by the remaining elastic portion of the web around the neutral axis (Case 2). For any given stage of yielding, the appropriate relationship between

---

[7] Joint Committee of the Welding Research Council and the American Society of Civil Engineers, Commentary on Plastic Design in Steel, 1961, p. 37.

the plastic moment, M_{ps}, as modified by shear and the full plastic moment, M_p, can be determined by consideration of the M-ϕ relationship and the shear stress distribution for that stage. However, the implied reduction in moment capacity does not actually occur because of strain-hardening.

Because of the stress concentrated at these points of interaction, strain-hardening is possible. Interaction between bending and shear occurs only when both types of stresses simultaneously reach high values. Since high shear and moment values occur in very localized zones of steep moment gradient, the beneficial aspects of strain-hardening usually enable the moment to reach the full plastic value. Therefore, in a tri-plate beam, no reduction in the plastic moment, M_p, is necessary if the value of the shear at the ultimate load does not exceed V_p, as given by equation (19).

The presence of shear has both a detrimental and a beneficial aspect. The beneficial aspect is due to the fact that shear forces always imply a moment gradient and, therefore, only a short girder portion is affected by the maximum moment. The adverse aspect is that a web which has yielded in shear cannot take its allotted bending moment and the flanges will have to compensate for it, resulting in excessive deflection and loss of load carrying capacity of the beam.

Deflection

Although strength to carry the load is the primary matter of importance in most structures, certain problems related to deflections can be of major concern. The deflection may exceed established limits

set up by a building code or specification. Excessive deflections may hinder the operation of moving parts or they may cause the cracking of plaster in finished ceilings. Thus, it is desirable to establish a method for calculating the deflections for a tri-plate beam and not to exceed recommended values established by existing codes.

In the elastic range, deflection of a flexural member varies inversely with the moment of inertia. In an I-shaped member the flanges account for most of the moment of inertia since they are farthest from the neutral axis. When high strength steel is used for the flanges, their area is reduced to such an extent that the moment of inertia of the section is reduced to a value that may be inadequate for deflection purposes.

The theoretical deflection at the center line of a beam loaded by symmetrical four-point loading is

$$\Delta = \frac{63PL^3}{EI} \times 10^{-3} \qquad (20)$$

where

Δ = the centerline deflection in inches

P = the load

L = the span length in inches

E = the modulus of elasticity of steel in psi

I = the moment of inertia of the section in inches to the fourth power

For the details of the derivation of equation (20) see Appendix B.

The use of a relatively small moment of inertia in this formula might result in excessive deflections. Specifications usually establish

a certain minimum depth-to-span ratio which serves to control deflection.

For a given uniformly distributed live load, the deflection of a beam is

$$\Delta = K_1 \frac{w_L L^4}{EI} \tag{21}$$

where

K_1 = a constant incorporating the end restraint

w_L = the uniformly distributed live load

The total load, including the effect of live load, creates a bending stress of

$$\sigma = \frac{Mc}{I} = K_2 \frac{w_T L^2}{I} \frac{d}{2} \tag{22}$$

where

K_2 = a constant of end restraint

w_T = the total uniformly distributed load

d = the depth of the beam

Combining equations (21) and (22) to eliminate I gives

$$\frac{d}{L} = 2 \frac{K_1 \, w_L}{K_2 \, w_T} \frac{\sigma}{E} \frac{L}{\Delta} \tag{23}$$

Consideration of the high level of stress developed in tri-plate beams and the deflection limitations established by various specifications indicates that equation (23) will yield relatively large span-to-depth ratios for high strength steel. Large d/L ratios require rather deep girders. However, if the live load is considered to be 50 percent of the total load, the span-to-depth ratios will be reduced to values

which are in line with present practice; i.e., smaller depths can be considered.[8]

Deflections of members in the plastic range can be obtained by integration of the basic differential equation:

$$\frac{dy^2}{dx^2} = \phi \qquad (24)$$

where

x = the distance along the member

y = the deflection from the original straight line of the member

$\frac{dy^2}{dx^2}$ = the approximate curvature of the member

ϕ = the curvature caused by bending

The use of equation (24) in the plastic range depends on the assumptions made in the moment-curvature relationship and on the methods of handling boundary conditions.

The problem of calculating deflections for tri-plate beams might be generalized by the following statement:

> In spite of the differences in the design basis, the working loads for both plastically designed beams and those designed by the allowable stress procedure are usually in the elastic range. Consequently, the calculation of deflection at working load is in general identical.[9]

The working load for tri-plate beams will be approximately halfway between the upper web yield moment and the upper flange yield moment in

---

[8] Toprac and Engler, p. 91.

[9] L. S. Beedle and Associates, Structural Steel Design, The Ronald Press Company, New York, 1964, p. 222.

Stage III. The deviation of the moment curvature curve from a straight line in Stage III is almost negligible until the moment approaches the yield moment of the flanges. This slight deviation indicates that yielding of the extreme fibers of the web does not greatly affect the curvature. This result is not surprising since the flanges are still under elastic conditions, and they control the curvature of the section. Consequently, the deflection of tri-plate beams at working loads can be calculated on the basis of elastic deflection theory.

CHAPTER III

LABORATORY VERIFICATION

Materials and Test Specimens

In order to provide an experimental check of the analysis, four beams were tested in the Civil Engineering Laboratories at South Dakota State University, Brookings, South Dakota. The beams were designed to fit, with the fewest modifications, the available testing equipment. Ease of handling was also a consideration.

The webs of all four beams were 1/4 inches by 13 inches A36 structural carbon steel. The top flanges of all beams were 4 inches wide by 3/8 inches thick A441 high-strength steel. The bottom flanges of beams TF-1, TS-3, and TS-4 were 2 inches wide by 3/8 inches thick "T-1" constructional alloy steel as shown in Figure 7. The bottom flange of beam HS-2, however, was 4 inches wide by 3/8 inches thick A441 steel, i.e., beam HS-2 was a hybrid beam. These dimensions and the distribution of material offer a comparison between the results obtained for the tri-plate beams and those of a hybrid beam. Table II gives the cross sectional dimensions and properties for each beam.

The overall length of all four beams was 20 feet with a span length for each beam of 19 feet. The beams were loaded as shown in Figure 1 to simulate, as much as possible, uniform loading conditions. No stiffeners were provided at either points of loading or at points of support.

Eight-inch, gage-length tension coupons were tested to determine the longitudinal mechanical properties of the plates that were used to

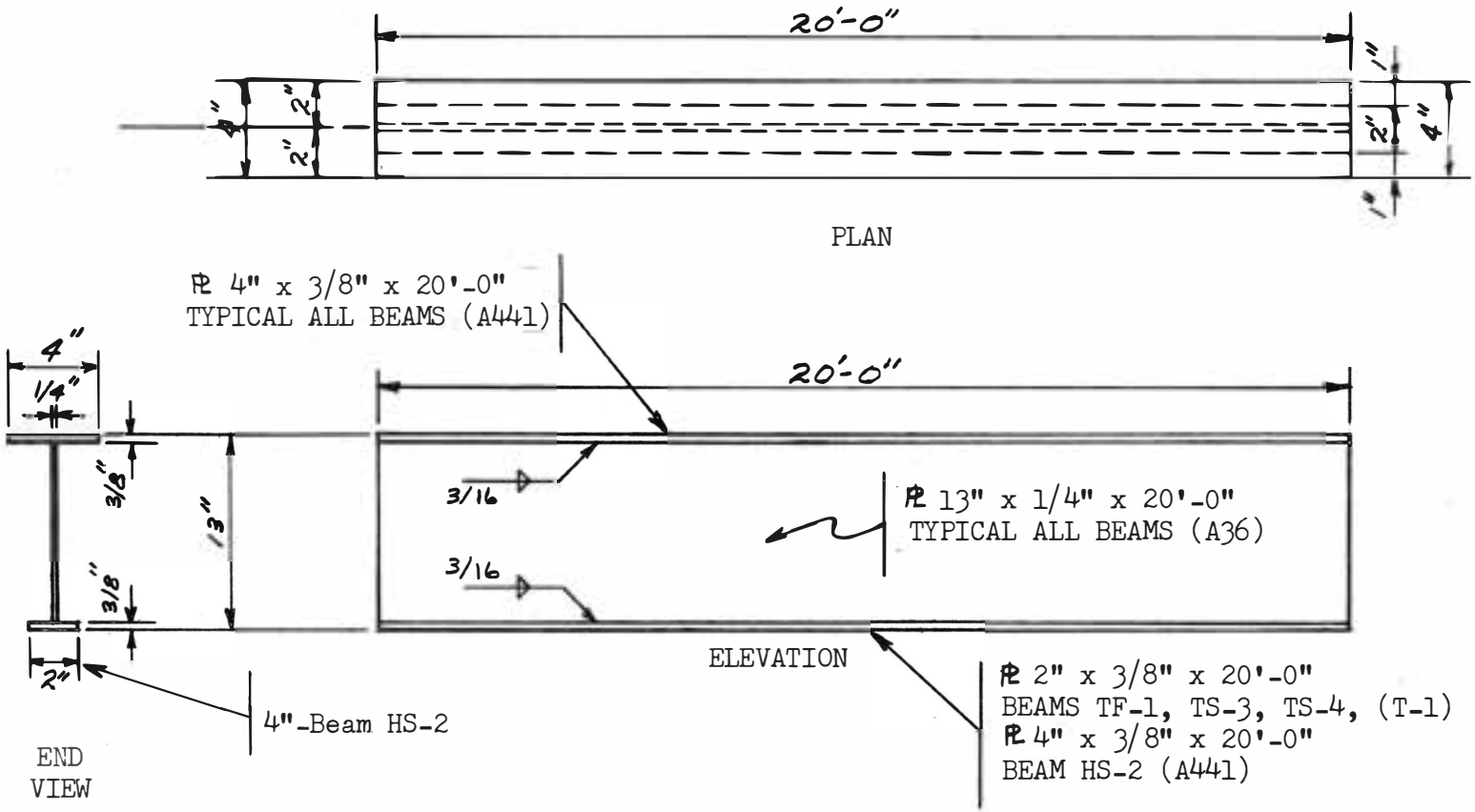

Figure 7. Details of Specimens TF-1, HS-2, TS-3, and TS-4

Table II

Dimensions and Sectional Properties of Test Beams

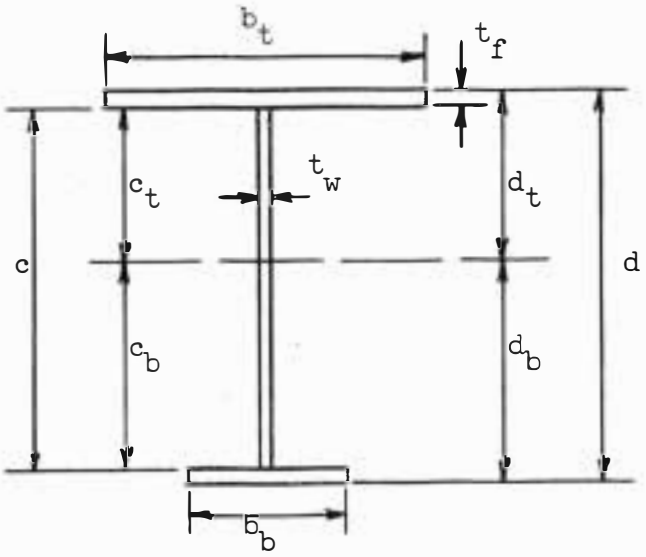

Beam	t_f inches	t_w inches	b_b inches	b_t inches	c inches
TF-1	0.378	0.262	1.987	3.985	13.014
HS-2	0.377	0.254	4.004	4.004	12.945
TS-3	0.379	0.260	1.993	3.990	13.011
TS-4	0.380	0.258	1.989	3.994	12.996

Beam	c_b inches	c_t inches	d inches	d_b inches	d_t inches
TF-1	7.399	5.615	13.770	7.777	5.993
HS-2	6.472	6.472	13.699	6.849	6.849
TS-3	7.402	5.609	13.769	7.781	5.988
TS-4	7.403	5.593	13.756	7.783	5.973

Beam	A $inches^2$	I $inches^4$	Z_w $inches^3$	Z_{fb} $inches^3$	Z_t $inches^3$
TF-1	5.666	142.039	11.302	8.741	5.699
HS-2	6.306	179.829	10.725	10.050	10.050
TS-3	5.650	142.075	11.213	8.767	5.731
TS-4	5.626	141.541	11.105	8.773	5.740

fabricate the test beams. The tension coupons were prepared from plate samples furnished by the fabricator. The averages of the results of the tension tests are listed in Table III. The average yield point for the web material of all beams was found to be 38,700 psi. The average yield point for the compression flange material, as well as the tension flange of beam HS-2, was 54,500 psi. The average yield point of the tension flange material of beams TF-1, TS-3, and TS-4 was found to be 109,300 psi. The bending properties of each beam, as calculated from the theoretical equations, are shown in Table IV.

Except at the ends, there was no flame cutting for all specimens. The flange to web connections were accomplished by a continuous partial penetration fillet weld using low-hydrogen electrodes, after the weld surfaces were mill surfaced.

Testing Procedure

A. Static Loading

All beams were simply supported six inches from each end. The static loading was applied at the fifth points of the span by four equal loads as shown in Figure 8. These loads were applied by using a single 60-ton hydraulic jack, located at the bottom of the testing machine and pulling the assembly through a high-strength steel bar. The dial on the manually operated pump read the psi pressure in the line. In order to interpolate the exact reading, the jack was calibrated by proving rings with the load applied by a compression testing machine. A jack factor of 11.4 was determined. The final preparation before testing was to

Table III

Mechanical Properties of Test Specimens
Yield Stress, Psi

Specimen	Web	Compression Flange	Tension Flange
TF-1	38,700	54,500	109,300
HS-2	38,700	54,500	54,500
TS-3	38,700	54,500	109,300
TS-4	38,700	54,500	109,300

Table IV

Bending Properties of Test Beams

Specimen	M_{y_1} ft-kips	M_{y_2} ft-kips	M_{y_3} ft-kips	M_{y_4} ft-kips	M_p ft-kips
HS-2	83.065	83.065	106.888	106.888	115.278
TS-3	55.479	75.919	94.567	113.104	116.292
TS-4	55.263	75.798	94.071	112.906	116.068

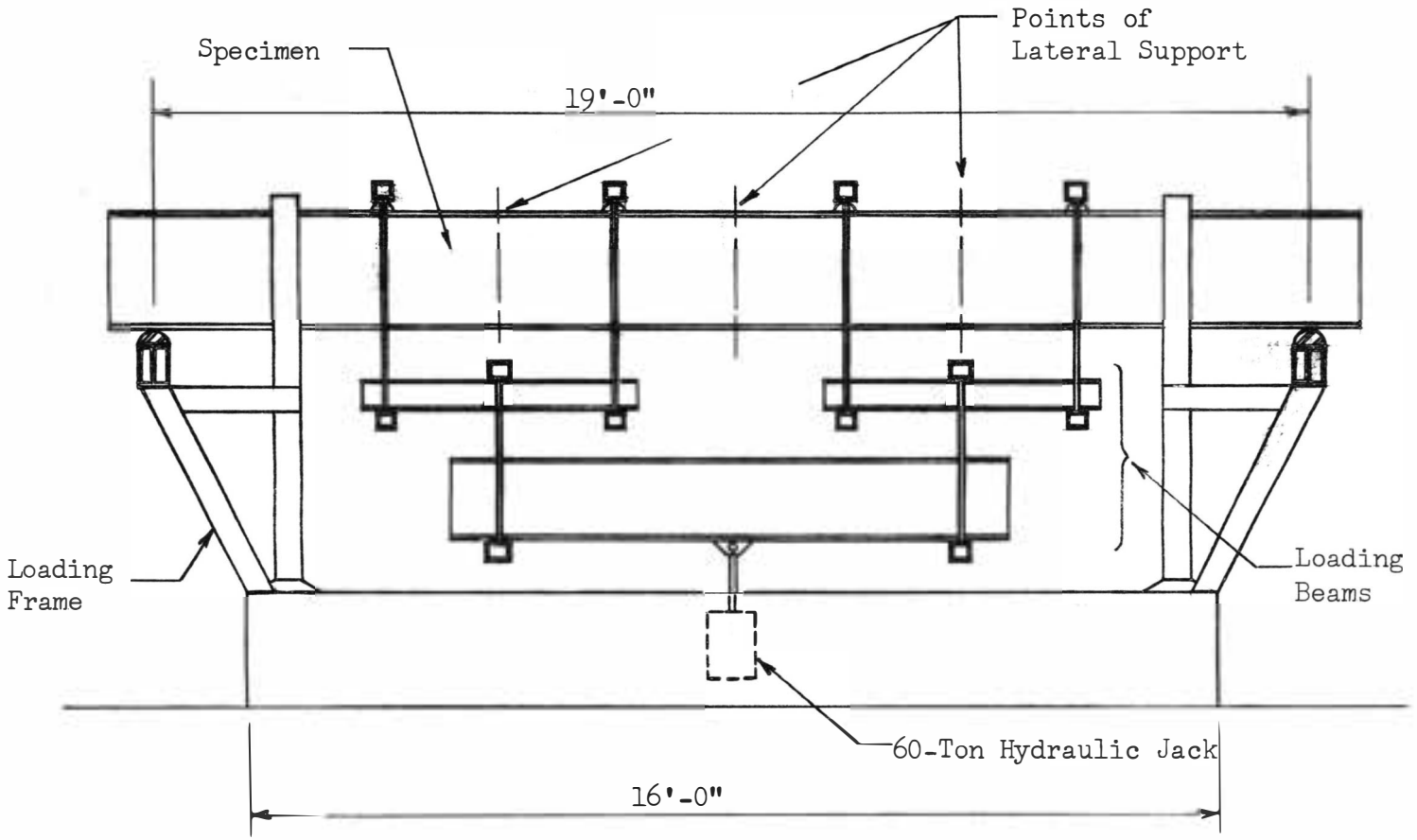

Figure 8. Test Setup for Static Load Tests

paint the specimens with lime whitewash in order to detect zones of yielding.

B. Fatigue Loading

The fatigue specimen was simply supported six inches from each end. The loading was applied at midspan by an automatically controlled hydraulic pump as shown schematically in Figure 9. The electrical control apparatus shown in Figure 10 controlled the rate of load application on the beam. Lateral bracing was provided at the points of support only. The test setup was as shown in Figure 11.

Specimen TF-1

Testing started with a 7,000 pound midspan load applied at the rate of eight cycles per minute; however, the load was later changed to 6,000 pounds so that the capacity of the apparatus would not be exceeded. A rate of loading greater than eight cycles per minute could not be maintained because of the limitations of the electrical control device. Strain gages were not provided for the fatigue testing.

The loading was carried on for varying periods of time with intermittent rest periods. Usually, testing continued for periods of 15 to 19 hours with rest periods between each series of load applications. However, at one point in the testing, the beam was idle for a period of several weeks because of equipment failure.

Investigations of the weld areas and checks on the deflection were conducted daily. A centerline deflection of 0.05 inches was

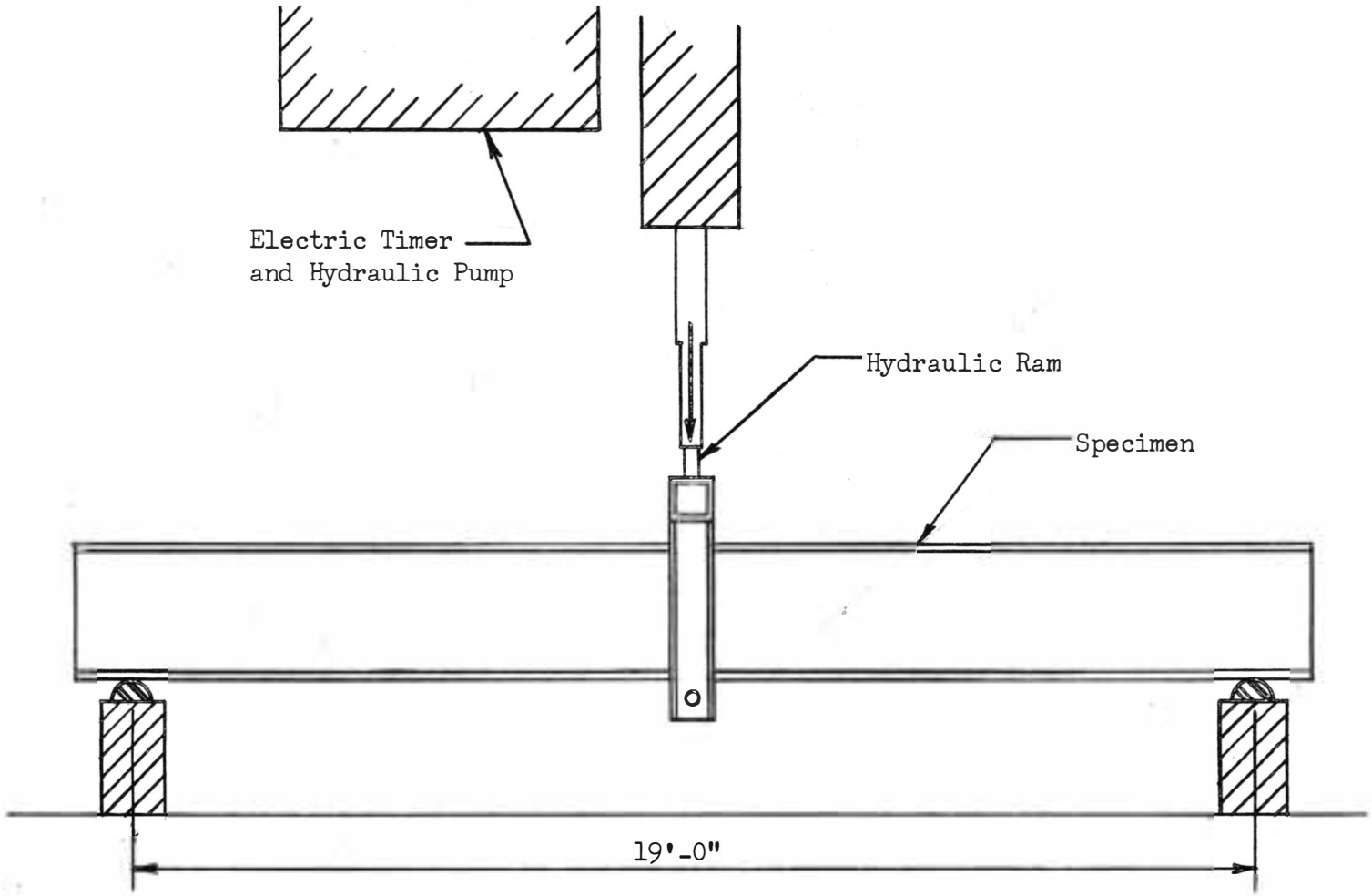

Figure 9. Test Setup for Fatigue Test

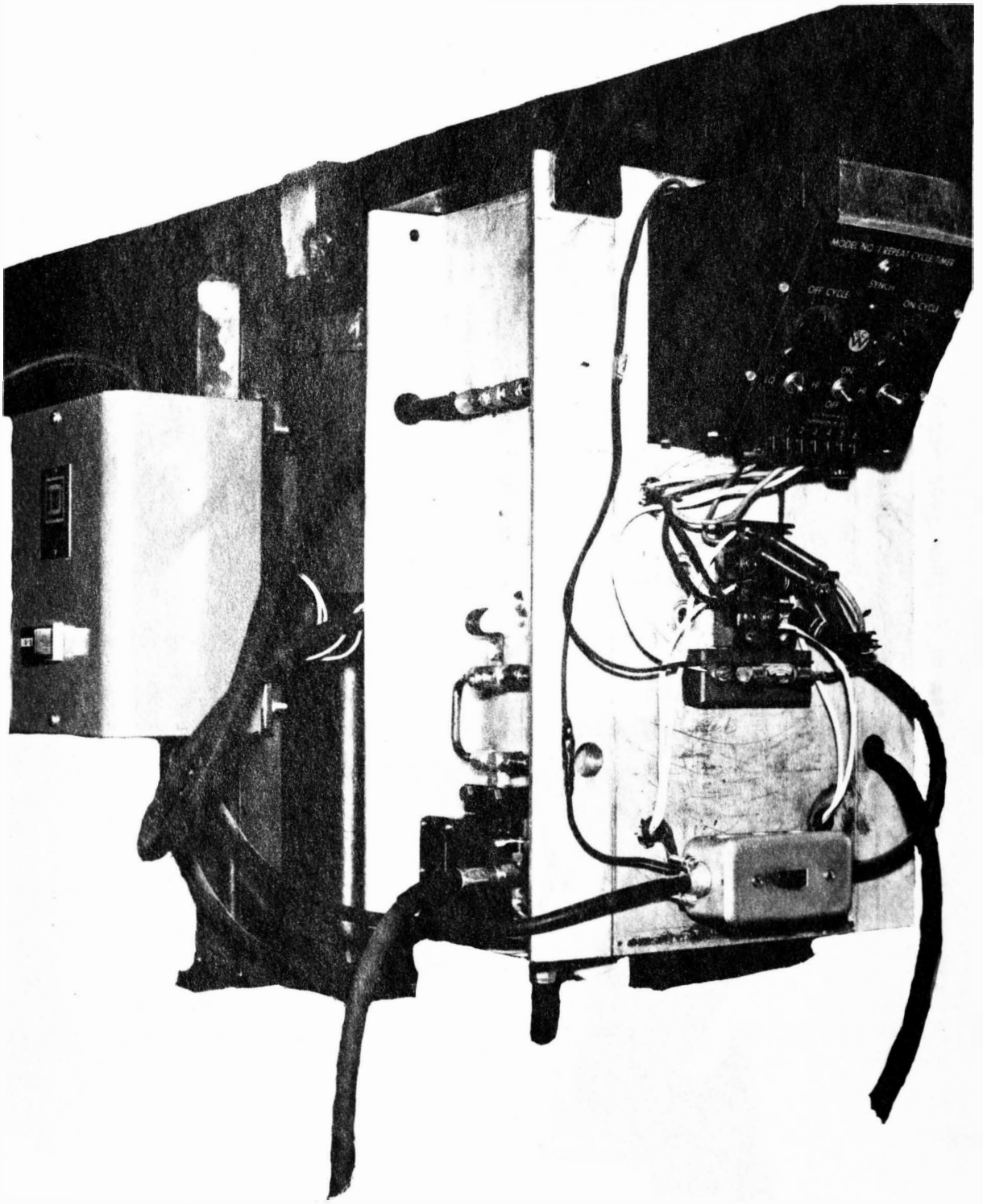

Figure 10. Electric Timer and Hydraulic Control Apparatus for Fatigue Testing Machine

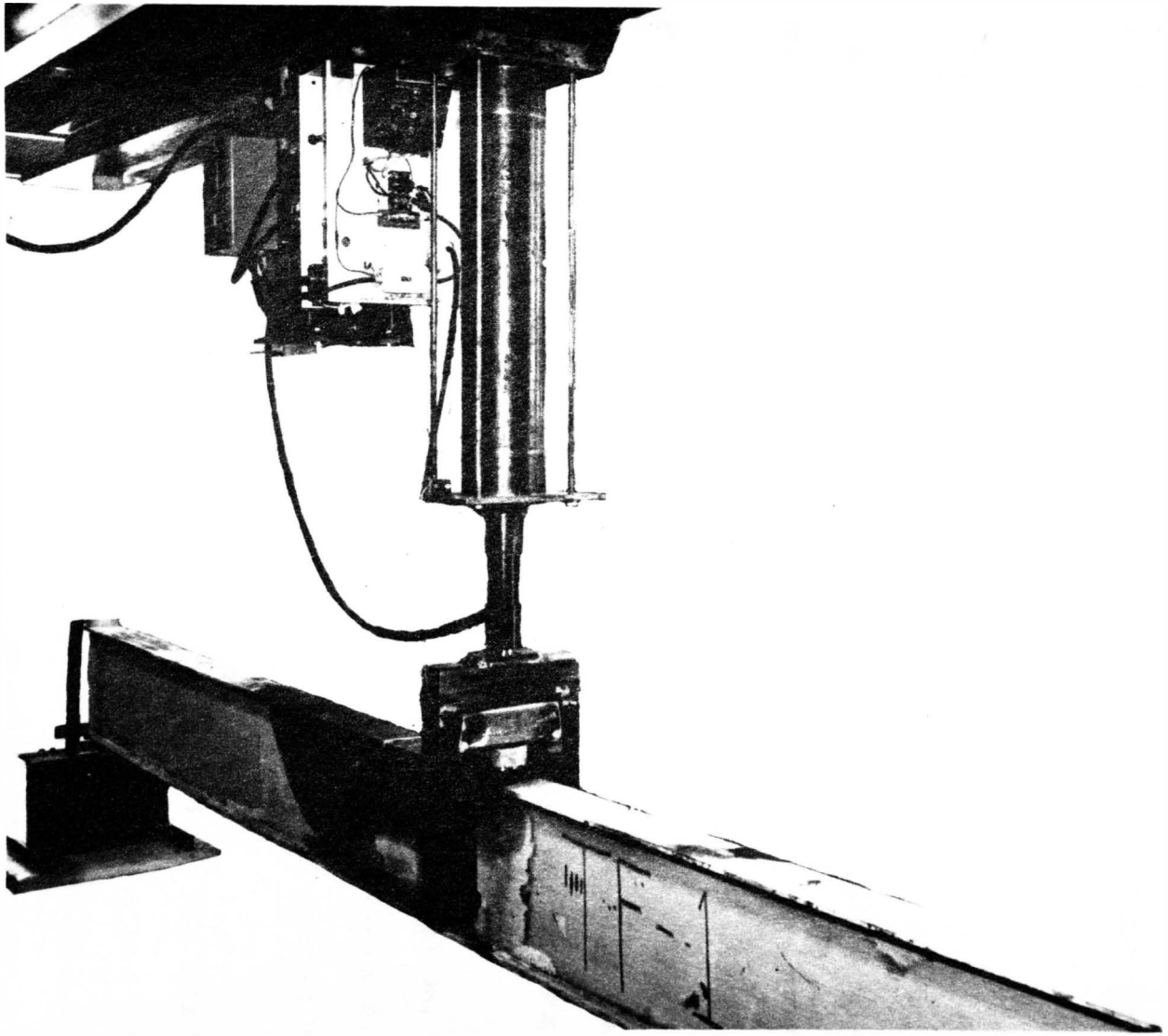

Figure 11. General View of Fatigue Test Setup

determined during the early loading and showed no change during the duration of the test.

Because of difficulties inherent in the testing equipment, the test was terminated after 232,067 cycles of loading had been applied to the beam. At this point, there was no indication of any impending failure.

Specimen HS-2

Beam HS-2 was the first specimen to be tested under static loads. Twelve SR-4 type A-1 strain gages were mounted on the beam. Figure 12 shows the location of these strain gages. All the strain gages were located at the center of the loading panels. The strain gages on the web were located two inches from either the top or bottom flanges. Strain gage number 5 was located at the neutral axis and strain gage number 3 was mounted on the opposite side of the web to give a running check of the readings at this point.

To prevent buckling before reaching the plastic condition, the beam was laterally supported at three points as shown in Figure 8. The apparatus used for lateral support is shown in Figure 13 and can be seen in the testing machine in Figure 14.

Figure 15 shows a general view of the test set up for this beam. The points of bearing between the lateral supports and the test specimen were heavily greased to minimize friction as the beam deflected vertically. The ends of the beam over the support had a clamp-type lateral support, as shown in Figure 15. Vertical deflection was measured by placing an Ames dial along the center-line of the beam under the bottom

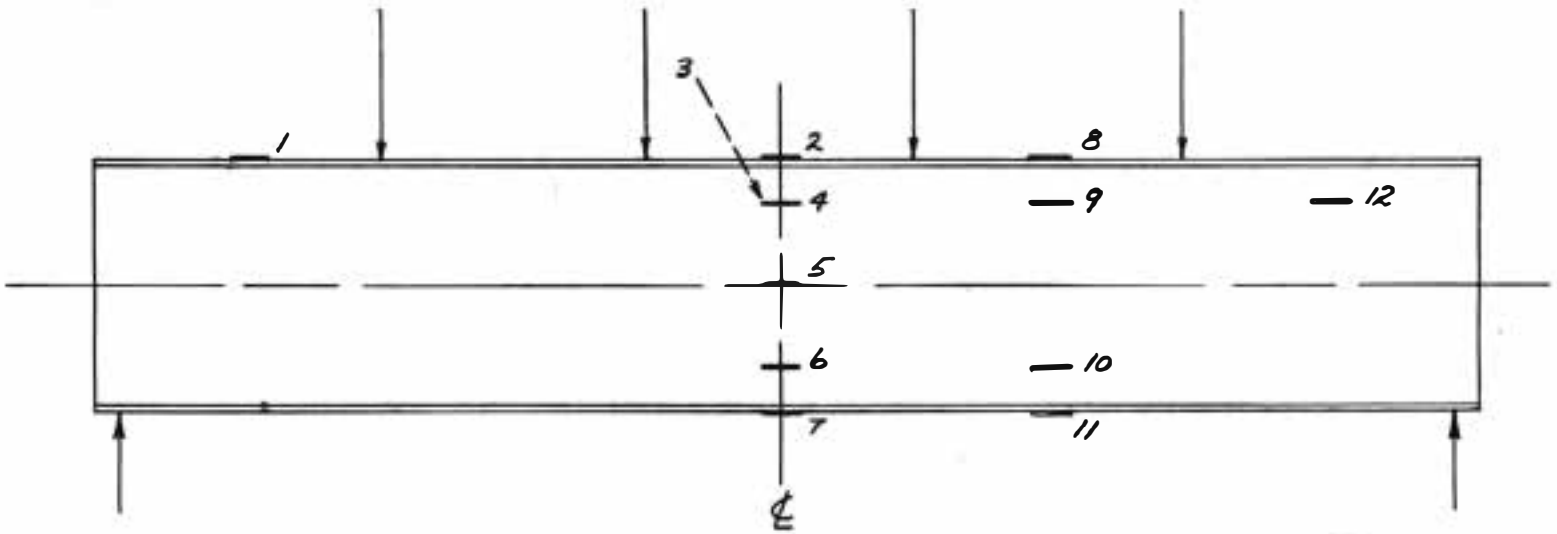

Figure 12. Strain Gage Arrangement
Specimen HS-2

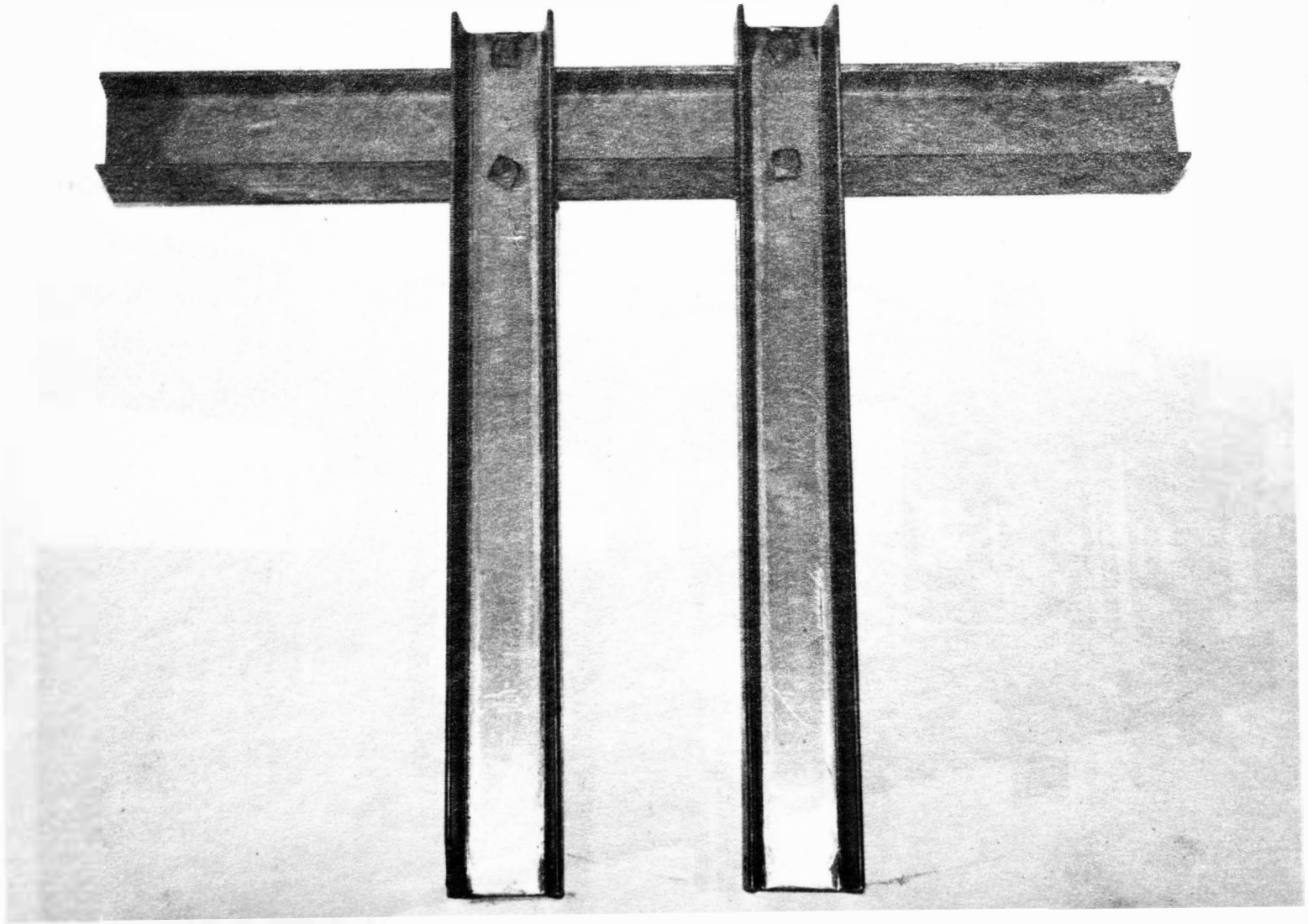

Figure 13. Lateral Support Device

flange. Lateral deflection was also measured by means of dial indicators located at intervals along the upper part of the web.

Testing started by loading the test specimen with a 5,000 pound load and unloading without taking any readings of the strain gages or of the deflection dials. This loading was repeated three times. The reason for this loading and unloading was to release any residual stresses that may have resulted during fabrication of the beam. No attempt was made to measure the existing residual stresses, assuming that the loading-unloading process would virtually eliminate their effect.

The beam was then loaded to a moment of 42.123 ft-kips which corresponded to 14,780 pounds of actual loading. This moment and load include the weight of the beam and the weight of the assembly hanging on the beam. The pump dial readings and the corresponding loads and moments for each beam are given in Appendix C. Because of the weight of the assembly, the deflection curves do not start from zero load. The load was applied at 2,280 pound intervals. At the end of every interval the loading was stopped and readings were recorded for the strain gages and deflection dials. The lateral supports were also frequently checked to see if they were functioning properly. When a moment of 42.123 ft-kips was reached, a final reading was taken and the beam was unloaded. During this cycle of loading, the moment applied was considerably below the web yield moment, M_{yw} = 83.065 ft-kips; and the beam behaved elastically, as expected. The strain gage readings for this first cycle of loading showed very close agreement with the linear strain distribution along the cross section.

The second cycle of loading was to load the beam beyond the web yield limit but short of the flange yield moment of 106.888 ft-kips, then to unload the beam and observe the amount of residual deflection resulting from yielding of the web. The load was applied at intervals of 2,280 pounds and readings were again taken at the end of each interval. The loading was continued until a moment of 94.107 ft-kips was reached, which corresponded to an actual load of 33,020 pounds. The beam was unloaded from the 33,020 pounds load and was noticed to behave elastically during the unloading. The vertical deflection dial read 0.167 inches when the load dial reading had returned to zero as shown in Figure 16.

A third cycle was attempted with 4,560 pound load intervals until a load of 23,900 pounds was reached. The load interval was then changed to 2,280 pounds. The loading was terminated when the moment on the beam slightly exceeded the flange yield limit of 106.888 ft-kips, but was below the theoretical plastic moment, M_p = 115.278 ft-kips. At this point, flaking of the whitewash became apparent on the upper web and flange. Inspection of the lateral supports showed them to be functioning properly. Since there was no apparent buckling in the beam, it was decided not to load any further but rather to unload the beam and observe the behavior of the beam during the unloading cycle. During the unloading the beam behaved elastically; when the final load reading showed zero, the amount of residual deflection was 0.269 inches.

A fourth and final cycle of loading was tried with the purpose of observing the maximum load carrying capacity of the beam. The beam was

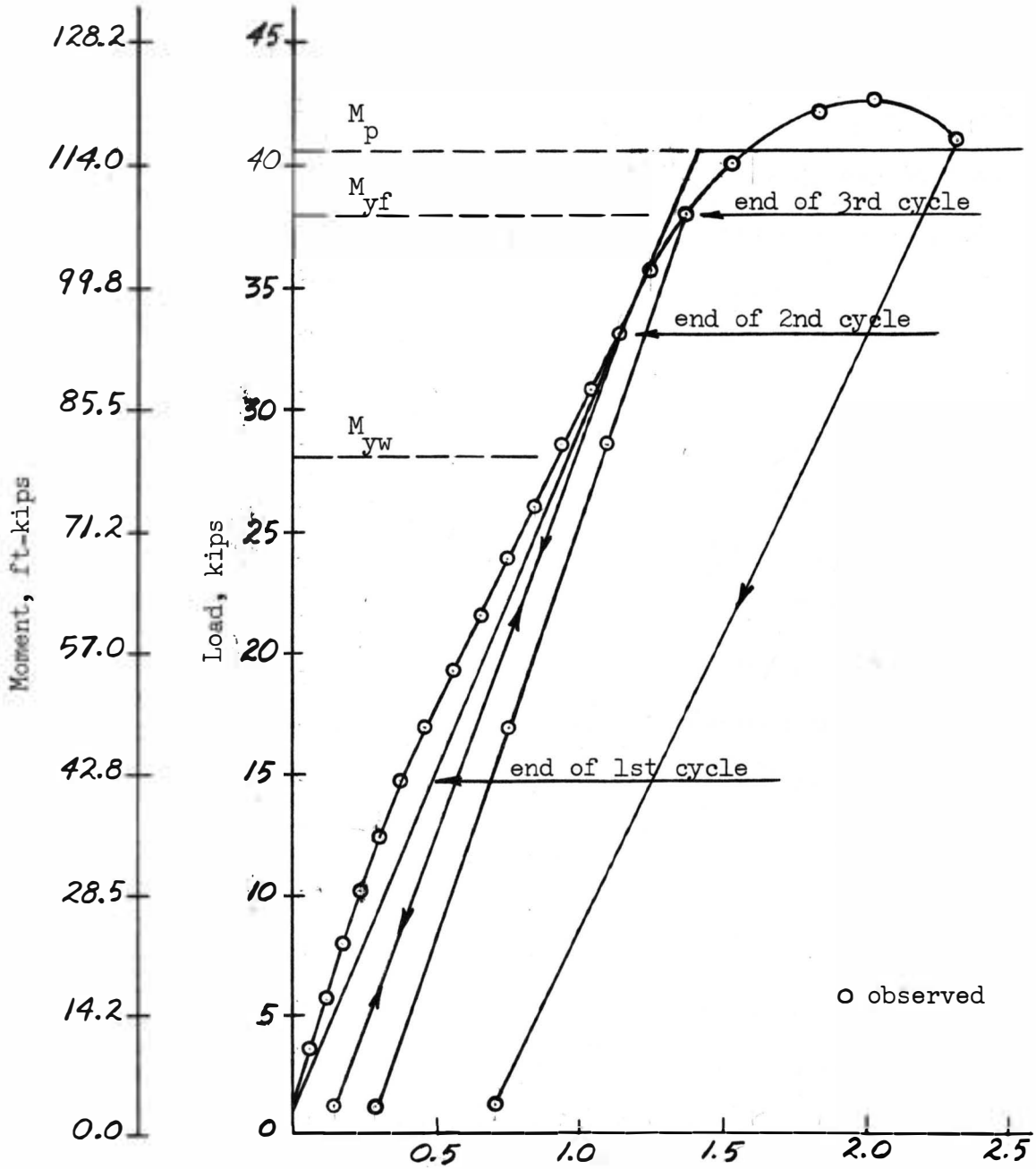

Figure 16. Load Versus Deflection at Midspan
Beam HS-2

loaded as in the previous cycle with readings taken at the end of each interval. Until a load of 42,140 pounds was reached, there appeared to be a few signs of buckling. However, as soon as the load exceeded 42,140 pounds, the deflection increased rapidly at a steady rate accompanied by a drop in load and lateral buckling of the compression flange appeared as shown in Figure 17. The highest load reached was 42,710 pounds. Figure 16 shows all test results for this beam.

Specimen TS-3

Fourteen strain gages were mounted on beam TS-3, as shown in Figure 18. Strain gage number 11 was placed at the neutral axis, and gages 4 and 9 were mounted on the opposite side of the web. Since the lateral support devices had functioned properly throughout the first test, no alterations of design were necessary. The test procedure was very similar to that of Specimen HS-2. The beam was whitewashed and loaded with 5,000 pounds and unloaded several times to release any residual stresses.

The purpose of the first cycle of loading was to load the beam up to, but not to exceed, the lower web yield moment of 55.479 ft-kips. The beam was actually loaded to a moment of 54.834 ft-kips at intervals of 2,280 pounds. At the end of every interval the lateral supports were checked and the strain gage and deflection readings were recorded. When a moment of 54.834 ft-kips was reached, final readings were recorded and the beam was unloaded. As expected, the specimen behaved completely elastic during the loading and unloading of the first cycle.

The second cycle started with the same load intervals and the same procedure of reading the gages as the first cycle. The intention

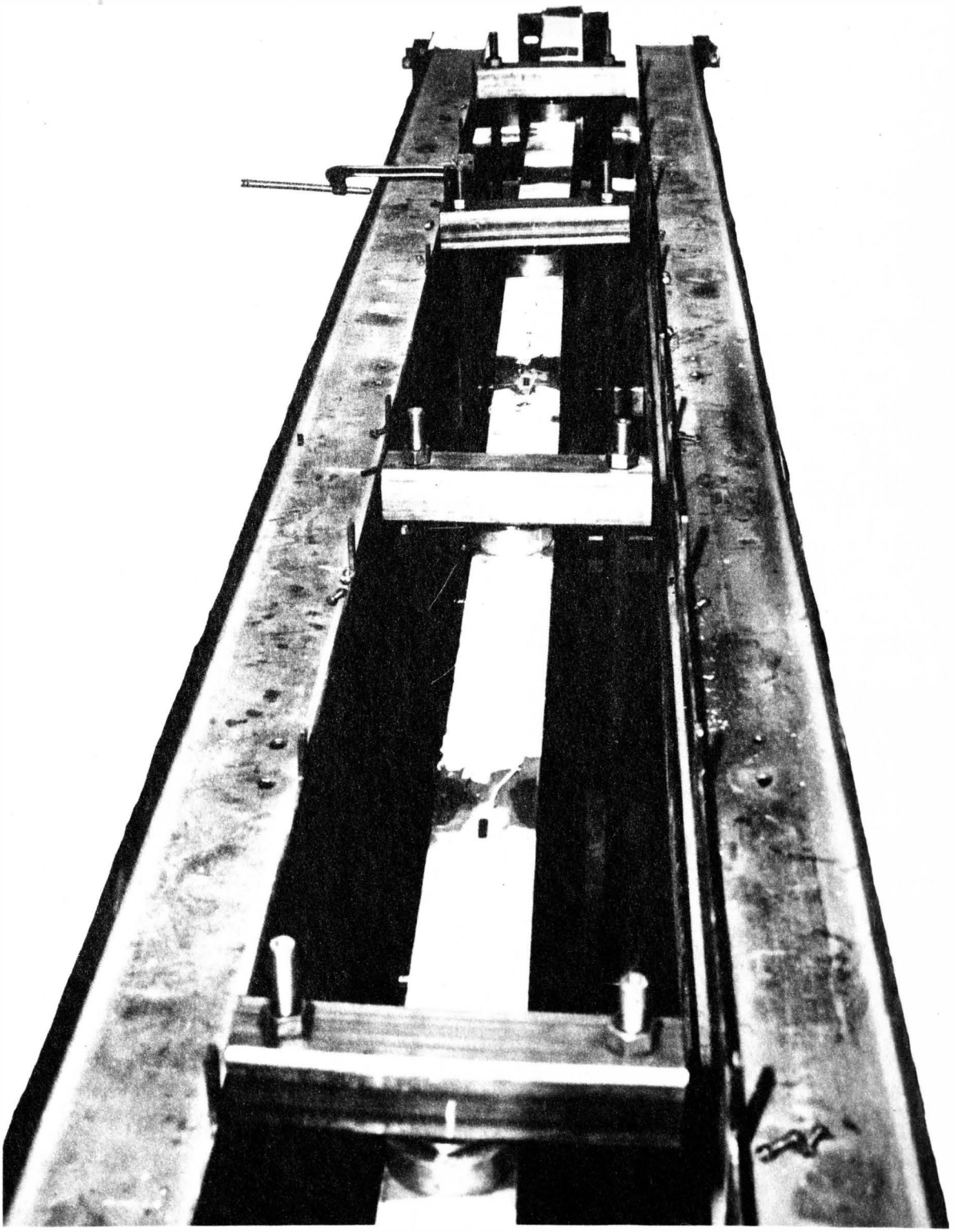

Figure 17. Lateral Buckling of Compression Flange of Specimen HS-2

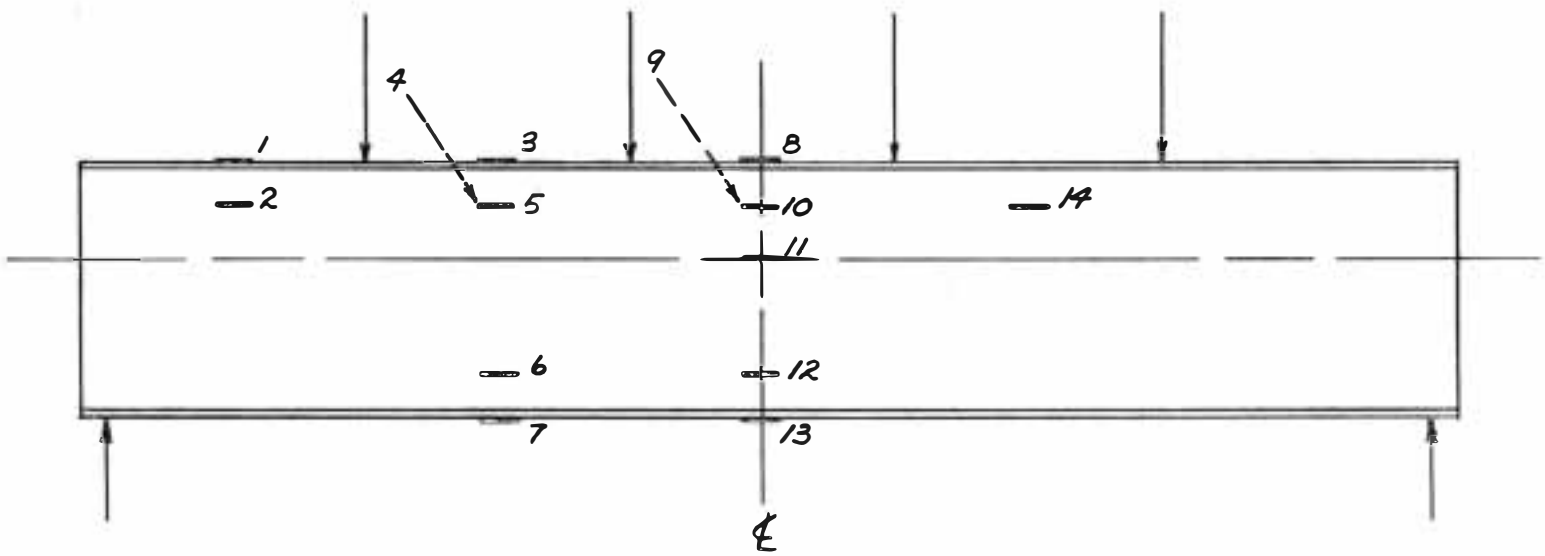

Figure 18. Strain Gage Arrangement
Specimen TS-3

of this cycle was to load the beam to a moment in excess of the web yield moment. However, as has been previously pointed out, the extreme fibers at the top and bottom of the web of the tri-plate beam do not begin yielding simultaneously. Yielding develops first in the bottom fibers with yielding in the extreme top fibers taking place at a higher level of stress. The loading continued until a moment of 61.332 ft-kips was reached. This moment exceeded the theoretical yield limit of the bottom fibers of the web, M_{y_1} = 55.479 ft-kips. At this point, it was decided not to unload the beam but rather to continue loading until the yield limit of the upper web fibers, M_{y_2} = 75.919 ft-kips, had been exceeded. The maximum moment attained at the end of this cycle was 80.826 ft-kips. Before unloading, a slight lateral deflection was indicated by the horizontal dials. There was also some evidence of white-wash flaking on the compression portion of the web. When the load had been completely released, the vertical deflection dial showed a residual deflection of 0.175 inches.

A third cycle of loading was started with intervals of 4,560 pounds. Strain gage readings were recorded as in the previous cycles. At a load of 19,240 pounds, the rate of applying the load was changed to 2,280 pounds. It was noticed that the beam behaved elastically and followed a straight line pattern that very closely coincided with the unloading of the second cycle. The path deviated from the straight-line pattern when the moment approached the theoretical plastic moment, as shown in Figure 19. When the moment on the beam reached 113.316 ft-kips, the horizontal dials indicated an excessive lateral deflection; it was

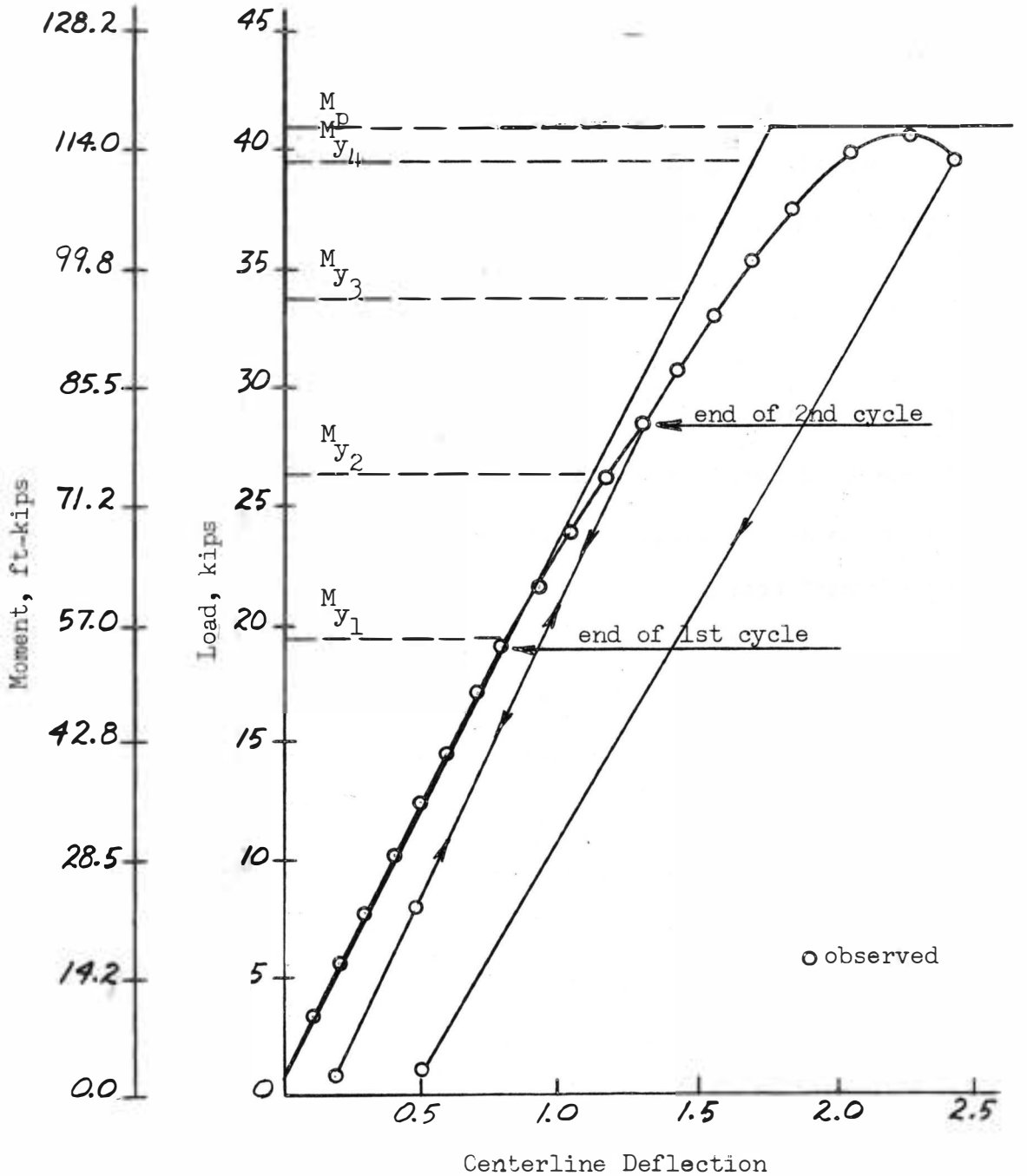

Figure 19. Load Versus Deflection at Midspan
Beam TS-3

noticeable that lateral buckling of the flange was impending. At this point, the vertical deflection was recorded as 2.05 inches. An attempt was made for another load interval, but at a load only slightly above 39,760 pounds, the compression flange buckled laterally, as shown in Figure 20; the vertical deflection increased rapidly as the load decreased. When the load dial was back to zero, the reading on the vertical deflection dial was 0.492 inches.

Specimen TS-4

The third specimen to be tested under static load was beam TS-4. Fourteen strain gages were mounted on this beam as shown in Figure 21. Three of the strain gages were placed on the opposite side of the web of this beam. Strain gage number 5 was located four inches from the top flange, and gage number 10 was mounted at the neutral axis.

The first step was to load the beam to a moment of 41.838 ft-kips. The rate of loading was 2,280 pound intervals, at the end of which strain gage and deflection readings were taken. Final readings were recorded at a moment of 41.838 ft-kips and the beam was unloaded. At the end of the loading and unloading of this first cycle the reading of the vertical deflection dial was 0.000 inches.

The procedure for the second cycle was exactly like that used for Specimen TS-3. The beam was first loaded to a moment of 61.332 ft-kips at intervals of 2,280 pounds. This moment exceeded the yield limit of the bottom fibers of the web, M_{y_1} = 55.263 ft-kips. Loading was continued until the load on the beam was greater than the yield moment of the upper web fibers, M_{y_2} = 75.798 ft-kips. The beam was actually

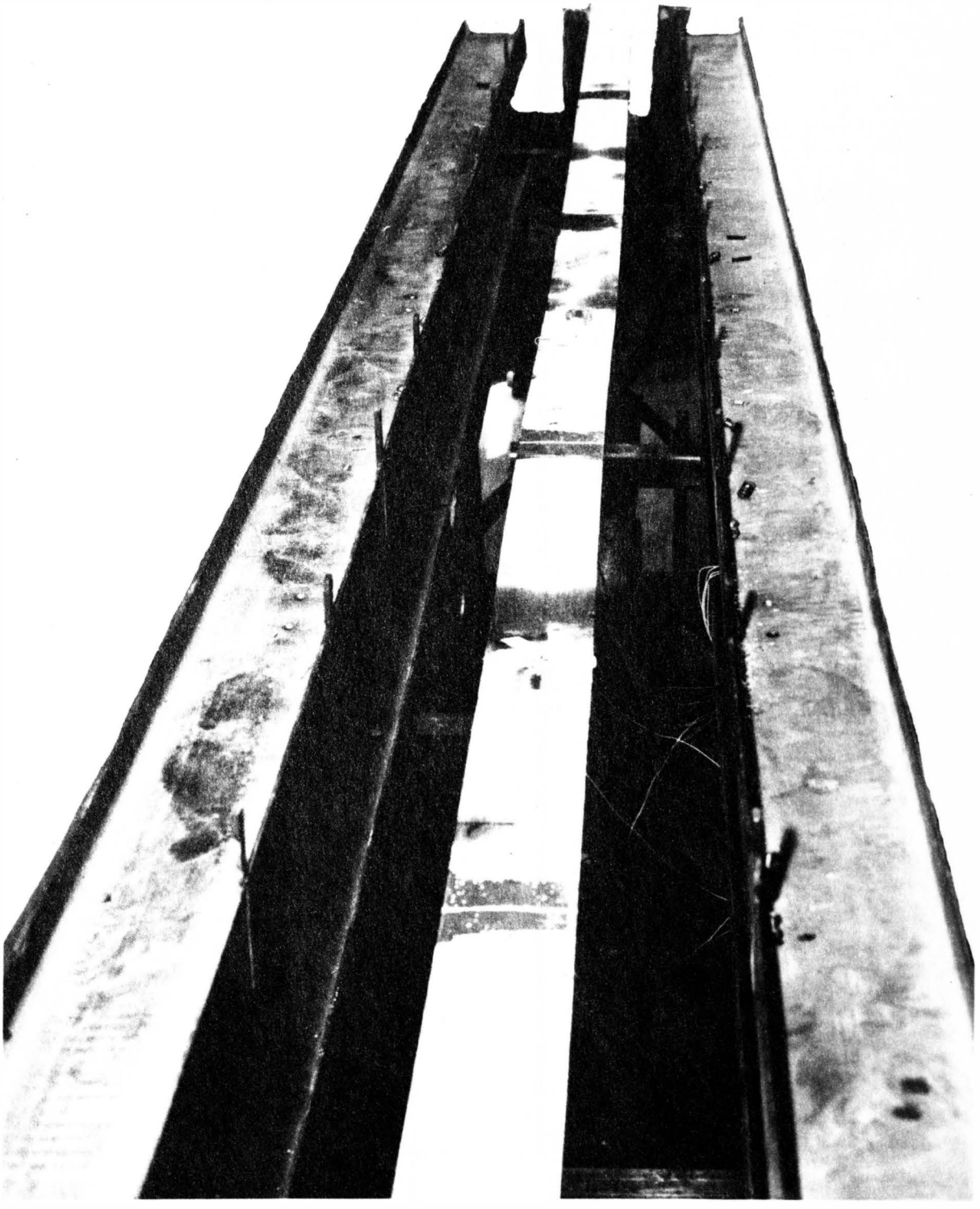

Figure 20. Lateral Buckling of Compression Flange of Specimen TS-3

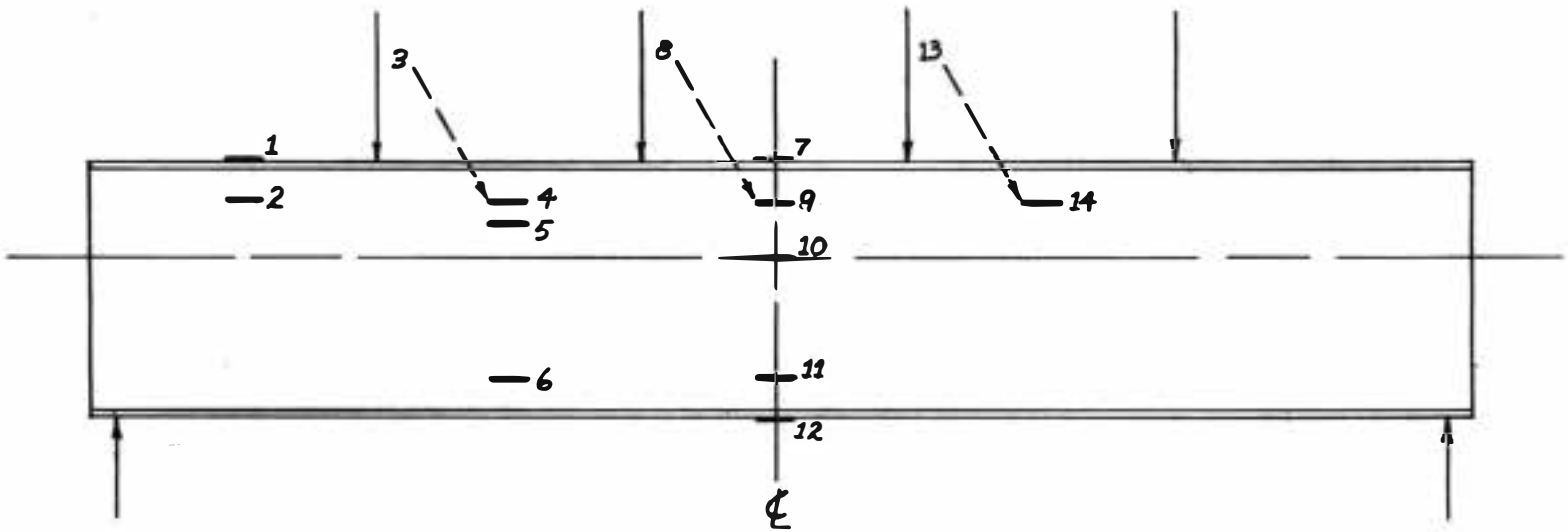

Figure 21. Strain Gage Arrangement
Specimen TS-4

loaded to a moment of 87.324 ft-kips. Before unloading, the horizontal dials indicated some lateral movements; however, after unloading, these dials returned to their initial readings. The residual vertical deflection after unloading the specimen was 0.199 inches.

A third cycle was tried with the purpose of reaching the theoretical plastic moment limit. As with beam TS-3, the loading of the third cycle coincided with the unloading of the second cycle, as is shown in Figure 22. At a load of 37,480 pounds, the lateral deflection became quite pronounced. When the load exceeded 39,760 pounds, the deflection rate started increasing steadily and the lateral flange buckling appeared as shown in Figure 23. The highest load reached was 40,900 pounds, which corresponded to a moment of 116.565 ft-kips. This moment was just above the theoretical plastic moment of 116.068 ft-kips. When the load dial read zero, the reading of the vertical deflection dial was 0.622 inches. The flaking of the whitewash on the upper portion of the web in Zone A is shown in Figure 24.

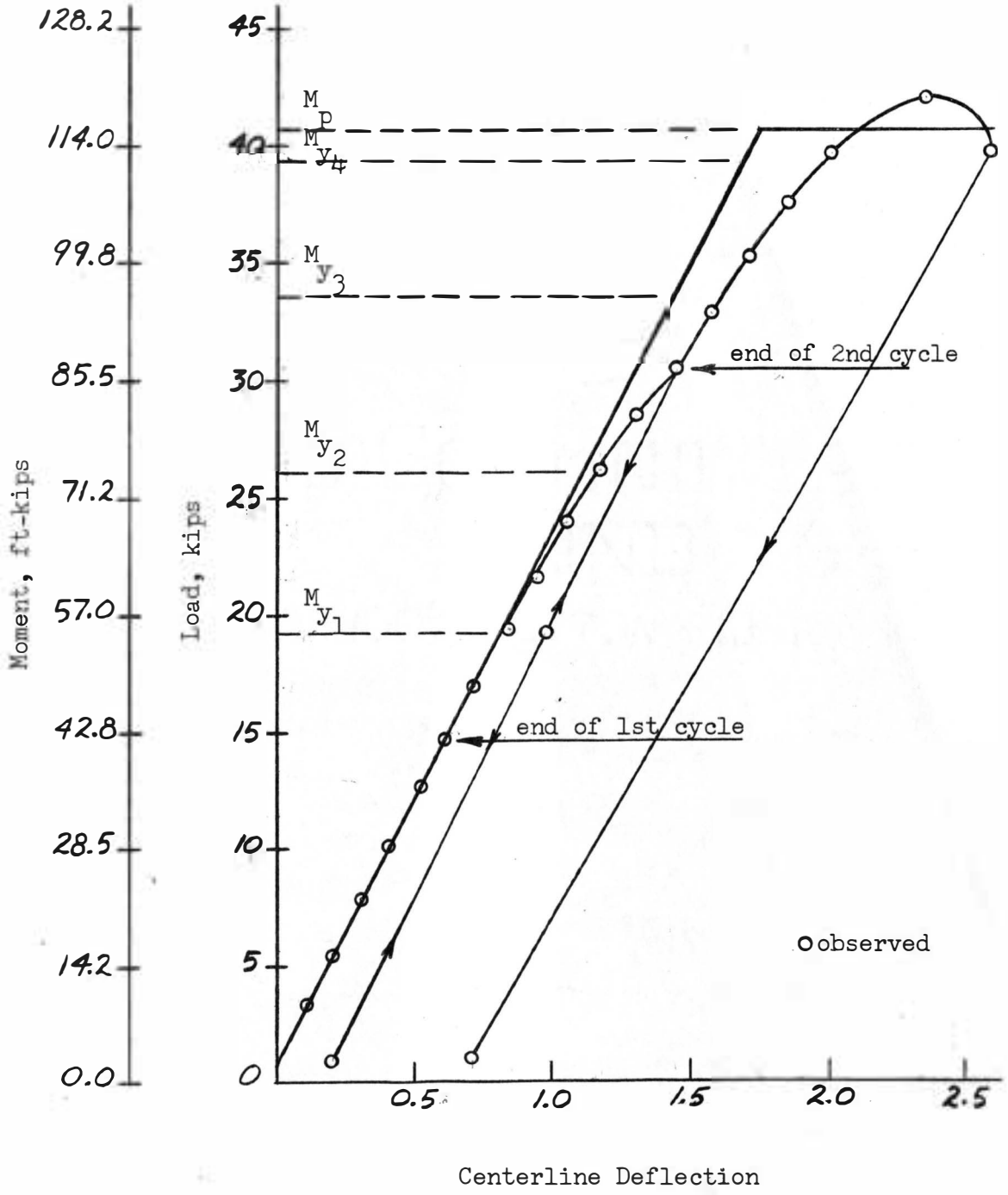

Figure 22. Load Versus Deflection at Midspan
Beam TS-4

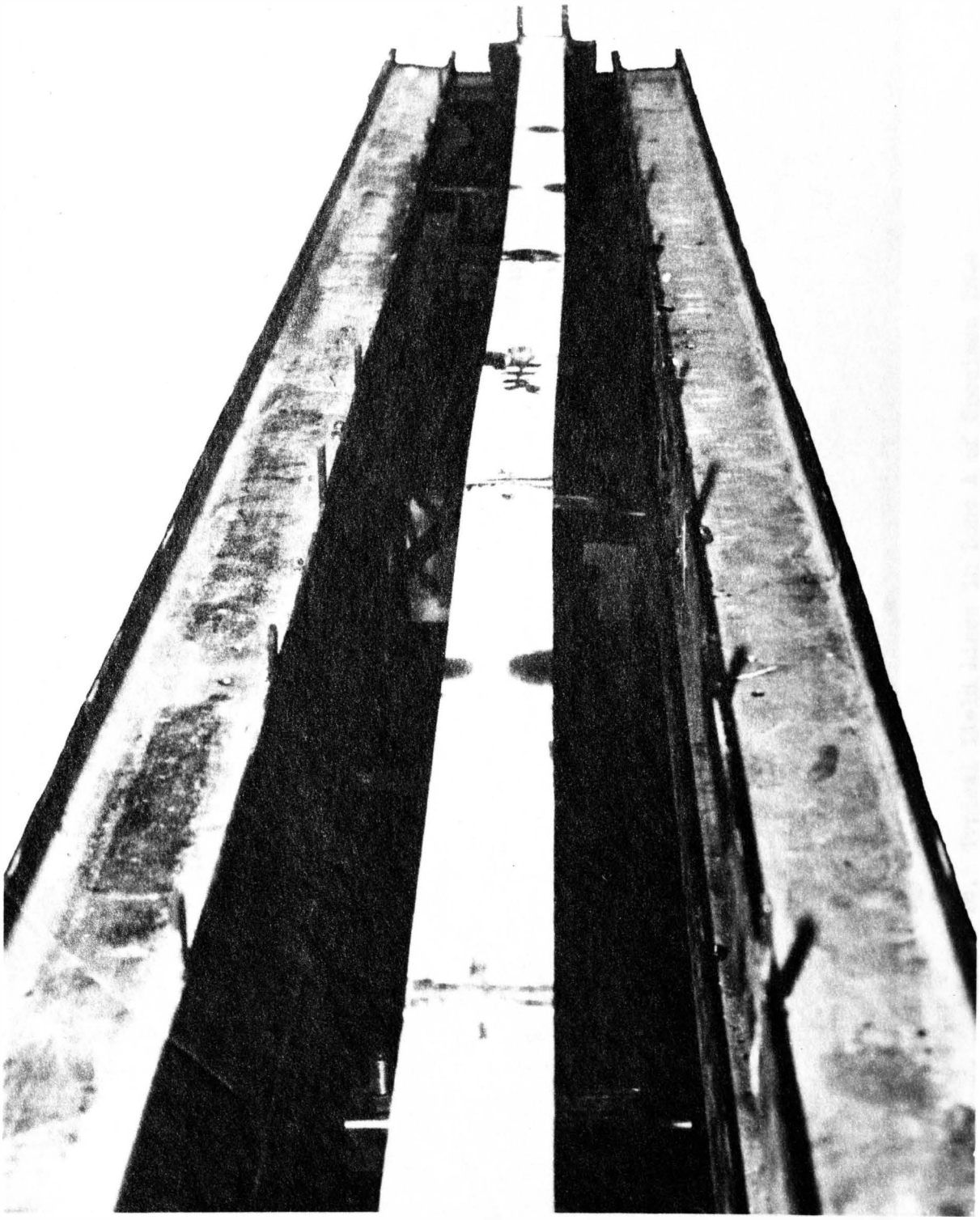

Figure 23. Lateral Buckling of Compression Flange of Specimen TS-4

Figure 24. Typical Yield Lines in Zone A of Specimen TS-4

CHAPTER IV

TEST RESULTS

Specimen TF-1

A goal of 1,000,000 cycles of loading was established for the fatigue test of Specimen TF-1. However, because of the relatively slow rate of load application and frequent mechanical problems with the testing equipment, only 232,067 cycles of loading were actually achieved.

Investigation of the stresses that were being developed in the section under the 6,000 pound midspan load indicated that they were considerably less than the yield stresses of the three steels used in the beam. However, this was not considered significant since a member may fail after a certain number of load applications even if the maximum stress in a single cycle is much less than the yield stress of the material.

It was expected that high stresses in the vicinity of the welds would develop which would reduce the permissible repeated range of stress for failure. Fatigue failure was expected to initiate at a flaw in the flange-to-web fillet weld and propagate through the flange and into the web. However, daily checks of the deflection and of the weld areas gave no indication of an impending failure or of a change in the elastic properties of the beam. Since such a small number of load applications was achieved, it was virtually impossible to draw any significant conclusions concerning the fatigue properties of tri-plate beams.

Specimen HS-2

During the loading and unloading of the first cycle, the beam behaved elastically following a straight line relationship on the deflection versus load curve, Figure 16. The second cycle also indicated elastic behavior, and the observed deflection curve followed the same path traced by the deflection points of the first cycle of loading. However, the observed deflections for both cycles were less than the theoretical deflection. This deviation may be attributed to some restraint from the lateral supports. Although the lateral supports had been heavily greased, it was noticed that some partial binding was occurring between the lateral supports and the tension flange. This problem was easily corrected, and no further problems were encountered.

The observed load-deflection curve for the third cycle of loading followed the path of the unloading of the second cycle. Although the third cycle was not terminated until the moment had reached the calculated flange yield limit, the residual deflection after unloading this cycle was relatively small. This residual deflection was 0.0011 of the span length.

The load-deflection curve for this test indicates elastic behavior far above the yield point stress in the web. Actually, the deflection curve did not deviate appreciably from a straight line relationship until a moment value in excess of the flange yield moment was reached. Also, at this point, the observed deflection became greater than the theoretical deflection.

The approximate analysis indicated a plastic moment of 115.278 ft-kips for this beam. When the theoretical plastic limit was reached,

distinct yield lines were observed on the upper web and flange; it was evident that buckling of the compression flange was impending. Upon increasing the load, the compression flange buckled laterally in Zone A. This yielding occurred in the region indicated by calculation, but at a higher load. Assuming the calculated plastic moment to be a measure of the ultimate strength, the specimen carried 5 percent more moment than calculated.

This test demonstrated that there is little adverse effect on the ultimate carrying capacity of a hybrid beam when the web of the member is stressed beyond its yield strength. In fact, the load-deflection curve indicates elastic behavior throughout a wide load range. These results compare favorably with the results of the previously mentioned tests on the behavior of hybrid beams.

Specimen TS-3

During the first cycle of loading, the beam behaved elastically, as expected. Since the frictional resistance of the heavily greased lateral supports had been virtually eliminated, the centerline vertical deflection during this cycle was in very close agreement with the theoretical deflection as shown in Figure 19. The initial loading of the second cycle indicated a load-deflection curve coincident with that of the first cycle. This coincidence was as expected, since this loading was well within the elastic range.

The approximate analysis indicated first yielding would occur in the lower web of Zone A at a moment of 55.479 ft-kips. First flange

yield was calculated to occur in the compression flange of Zone A at a moment of 94.567 ft-kips.

The first yield lines were observed in Zone A during the upper limits of the second cycle of loading. Although the second cycle was not terminated until the yield limits of both the bottom and top web fibers had been exceeded, the only evidence of yielding was in the compression portion of the web. This yielding did not seem to influence the behavior of the beam because no significant change in deflection was evident in the load-deflection curve until after the yield limits of the web material were exceeded.

During the loading of the third cycle, the beam behaved elastically and followed a straight line pattern that very closely coincided with the unloading of the second cycle. This path deviated from the straight line relationship when the loading reached the calculated yield limit of the flanges. At this stage, flaking of the whitewash indicated yielding in the compression flanges. There was little evidence of yield lines in the tension flange.

A slight buckling of the compression flange was visible at a moment of 113.316 ft-kips. At a moment of 115.539 ft-kips, the compression flange buckled laterally, representing 0.7 percent deviation from the theoretical plastic moment of 116.292 ft-kips. There was considerable whitewash flaking, with particular concentrations in Zone A.

The load-deflection curve, Figure 19, points out that at loads above the theoretical yield limits of the web, the observed deflections are considerably greater than the theoretical deflections. The centerline

deflection which was recorded just before failure represents an actual deflection 15 percent greater than calculated.

Specimen TS-4

The first cycle of loading on beam TS-4 was completely elastic without any residual deflection at the end of the cycle. As with beam TS-3, the observed centerline deflection of the first and second cycles were coincident.

As the yield point of the web material was reached, the plot of deflection versus load deviated from a straight line, although no yielding was yet visible on the beam. After this increase in deflection at the upper stages of the second cycle, a straight line relationship between load and deflection was again apparent until the moment reached the yield limit of the flanges.

Unloading of the second cycle produced a residual deflection of 0.199 inches, which is equivalent to 0.00087 of the span length. This amount of residual deflection is relatively small; where the dead load comprises a major portion of the total load, this residual can be corrected by a very small cambering of the beam.

In the upper stages of the third cycle the vertical centerline deflection again showed a significant increase. Also, at this point the lateral deflection became quite pronounced, and yield lines were observed in the compression area of the specimen. Lateral buckling of the compression flange did not take place, however, until the theoretical plastic limit had been exceeded. This buckling occurred in Zone A,

as expected, but at a higher moment than indicated by the approximate analysis.

The strain gages showed a uniform linear strain across the section with a negligible reading on strain gage number 10 which was located at the neutral axis. When the flange buckled, the readings were not consistent with any particular pattern.

The load versus deflection curve, Figure 22, indicates very close agreement between the observed and the theoretical deflections at low values of moment. However, as the moment on the beam is increased, the actual deflections tend to become considerably greater than the calculated values.

The load-deflection curves for all tests show that behavior of the specimens was very nearly elastic throughout the entire load range. The important fact brought out by these tests was that the member continued to act elastically even after a considerable portion of the web had been yielded.

All specimens in these tests had deflections which were much larger than the allowable live load deflection as specified by AASHO (American Association of State Highway Officials) and AISC. These deflections are not surprising since almost all of the load in these tests could be considered as live load, which, as pointed out in the theory, would result in an inadequate depth-to-span ratio. However, this fact cannot necessarily be used as a measure of usefulness of the member since, in actual practice, the live load will normally be in smaller proportion to the total load and deflections will be considerably smaller.

The ability of the lateral bracing system to prevent premature lateral buckling was excellent. The rigidity of the lateral supports, coupled with the larger compression flange area, tended to resist lateral buckling in the tri-plate beams. Actually, this effect might be compared to composite beams where the slab furnishes lateral support for the compression flange. It has been suggested that the lateral buckling problem and the deflection problem encountered through the use of high-strength steel flanges can be resolved by using composite construction.[10] This method not only provides lateral support but also increases the moment of inertia of the section so that deflections can be controlled.

Since theoretical analysis indicated that the shear would not have any detrimental effect on reaching the plastic moment, it was expected that the beams would fail by lateral buckling of the compression flange. Although premature buckling was not a problem, lateral buckling was the mode of failure in all tests.

The high plastic moment value obtained in the test of Specimen HS-2 can be attributed to strain-hardening. The four cycles of loading applied in this test strained the beam through the plastic region far in excess of the elastic limit strain. In such cases, strain hardening occurs, and any further deformation will be accompanied by an increase in the stress capacity of the material.

---

[10] Toprac and Engler, p. 91.

CHAPTER V

SUMMARY AND CONCLUSIONS

Summary

The results of the preceding tests are summarized in Table IV, which gives the calculated theoretical moment and the observed ultimate moment:

Table IV

Theoretical Versus Observed Moment

Test	M_{yf}, in ft-kips	M_{y_4}, in ft-kips	M_p, in ft-kips	M_o^*, in ft-kips
HS-2	106.888	-----	115.278	121.723
TS-3	-----	113.104	116.292	115.539
TS-4	-----	112.906	116.068	116.565

*M_o is the observed plastic moment

Conclusions

From results gathered during the testing of the specimens, the following conclusions were drawn:

1. The theoretical analysis appears to give a valid prediction of the ultimate strength. The calculated values obtained from equation (16) compared favorably with the test results.
2. When a tri-plate beam is loaded so that the yield points of the upper and lower web are exceeded, a redistribution of

stress will occur and allow the beam to continue to deform elastically. As shown in Figures 19 and 22, the load-deflection curve deviated from a straight line relationship when the yield points of the upper and lower web were exceeded. However, upon further loading, a redistribution of stress occurred, and the member continued to behave elastically until the yield points of the flanges were reached.

3. Deflection and lateral buckling become more important when a tri-plate is used because of the reduction in flange cross section. As previously pointed out, excessive deflections were obtained in each test. Also, the mode of failure for each beam was by lateral buckling of the compression flange.

4. The use of tri-plate beams was shown to be feasible. The beams tested developed an ultimate moment in the range of the calculated plastic strength, M_p.

5. The load carrying capacity of tri-plate beams is approximately equal to the ultimate strength of hybrid beams, as seen from the tests. If there is a small price differential between "T-1" steel and A441 steel, it means that the tri-plate concept lends itself to a lighter and more economical section than the hybrid beam.

6. The upper practical limit of bending strength for design purposes is the moment causing initial yielding in the tension flange. Because it represents the moment above which the

curvature deviates significantly from a straight line, elastic rather than plastic design limitations can be used.

Recommended Areas of Future Study

The study of the behavior of tri-plate beams is relatively new and should be investigated more extensively in the following areas:

1. A more complete study of the fatigue properties of tri-plate beams should be undertaken.
2. Tri-plate beams with thin webs should be investigated with particular emphasis on the utilization and study of stiffeners.
3. The use of tri-plate beams in composite construction should be studied.
4. The shifting of the neutral axis in tri-plate beams, and the effect on the bending behavior, should be extensively analyzed.

NOTATION

The following notation is used in this thesis:

A = cross sectional area of the entire beam

A_w = cross sectional area of the web

b_b = bottom flange width

b_t = top flange width

c = web depth

c_b = distance from the neutral axis to the extreme bottom web fibers

c_t = distance from the neutral axis to the extreme top web fibers

d = beam depth

d_b = distance from the neutral axis to the extreme bottom flange fibers

d_t = distance from the neutral axis to the extreme top flange fibers

E = modulus of elasticity of steel

I = moment of inertia of the entire cross section of the beam

I_{fb} = moment of inertia of the bottom flange

I_{ft} = moment of inertia of the top flange

K_1 = constant of end restraint

K_2 = constant of end restraint

L = span length

M = bending moment

M_o = observed bending moment

M_p = plastic bending moment of the entire beam cross section

M_{yw} = bending moment at the initial yielding in the web (hybrid beam)

M_{yf} = bending moment at the initial yielding in the flanges (hybrid beam)

M_{y_1} = bending moment at the initial yielding of the lower web fibers (upper limit Stage I)

M_{y_2} = bending moment at the initial yielding of the upper web fibers (upper limit Stage II)

M_{y_3} = bending moment at the initial yielding of the upper flange (upper limit Stage III)

M_{y_4} = bending moment at the initial yielding of the lower flange (upper limit Stage IV)

P = concentrated load

t_f = flange thickness

t_w = web thickness

V = shear force

V_p = plastic shear of the web

w_L = uniformly distributed live load

w_T = total uniformly distributed load

x_b = distance from left support to Zone B

x_c = distance from left support to Zone C

y = distance from the neutral axis to the plane of stresses

Z = plastic modulus of the entire beam cross section

Z_{fb} = plastic modulus of the bottom flange

Z_{ft} = plastic modulus of the top flange

Z_w = plastic modulus of the web

Δ = centerline deflection

ϵ = strain

ϕ = curvature

σ = stress at the extreme fibers of the section

σ_y = yield stresses at the extreme fibers of the section

σ_{y_3} = yield stress of the upper flange

σ_{y_4} = yield stress of the lower flange

σ_{yw} = yield stress of the web

ρ = radius of curvature

τ = shear stress in the web

τ_y = shear yield stress of the web

W = total jack load

BIBLIOGRAPHY

1. Haaijer, G., "Economy of High Strength Steel Structural Members," Transactions, American Society of Civil Engineers, vol. 128, 1963.

2. Toprac, A. A., and R. A. Engler, "Plate Girders With High-Strength Steel Flanges and Carbon Steel Webs," Proceedings, American Institute of Steel Construction, 1961.

3. Frost, Ronald W., and C. G. Schilling, "Behavior of Hybrid Beams Subjected to Static Loads," Journal of the Structural Division, ASCE, vol. 90, no. ST3, Proceedings Paper 3928, June, 1964.

4. Sarsam, Jamal B., "Behavior of Thin Web Hybrid Beams Subjected To Static Loads," Master of Science Thesis, South Dakota State University, Brookings, South Dakota, August, 1965.

5. Joint Committee of Welding Research Council and the American Society of Civil Engineers, Commentary on Plastic Design in Steel, 1961.

6. Beedle, Lynn S., and Associates, Structural Steel Design, The Ronald Press Company, New York, 1964.

7. Gilligan, J. A., "Higher Strength Structural Steels," Civil Engineering, vol. 34, no. 11, November, 1964.

8. Beedle, Lynn S., Plastic Design of Steel Frames, John Wiley and Sons, Inc., New York, 1964.

9. Basler, K., "Strength of Plate Girders in Shear," Transactions, American Society of Civil Engineers, vol. 128, 1963.

10. Reneker, W. D., and C. E. Ekberg, "Flexural Fatigue Tests of Prestressed Steel I-Beams," Journal of the Structural Division, ASCE, vol. 90, no. ST2, Proceedings Paper 3868, April, 1964.

11. Basler, K., "Strength of Plate Girders Under Combined Bending and Shear," Transactions, American Society of Civil Engineers, vol. 128, 1963.

12. Stuessi, F., "Theory and Test Results on the Fatigue of Metals," Transactions, American Society of Civil Engineers, vol. 128, 1963.

APPENDIX A

DERIVATION OF MOMENT-CURVATURE RELATIONSHIPS FOR PURE BENDING

The moment-curvature relationship at any given stage of loading can be obtained by integrating the stress areas according to the general expression

$$M = \int_{Area} \sigma dAy$$

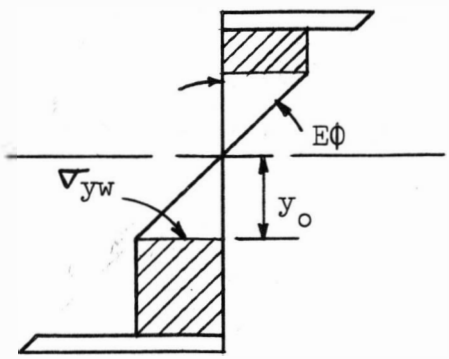

Stage II

$$M = \int_{A_f} \sigma dAy + \int_{y_o}^{c_b} \sigma_{yw} t_w dy \cdot y + 2\int_{0}^{y_o} \sigma t_w dy \cdot y$$

$$= E\phi(I_{ft} + I_{fb}) + \sigma_{yw} \frac{t_w c_b^2}{2} - \sigma_{yw} \frac{t_w y_o^2}{2} + 2\sigma_{yw} \frac{t_w y_o^2}{3}$$

$$M = E\phi(I_{ft} + I_{fb}) + \sigma_{yw} \frac{t_w c_b^2}{2} + \sigma_{yw} \frac{t_w y_o^2}{6}$$

where $$y_o = \frac{\sigma_{yw}}{E\phi}$$

Therefore

$$M = E\phi(I_{ft} + I_{fb}) + \sigma_{yw} \frac{t_w c_b^2}{2} + \frac{t_w \sigma_{yw}^3}{6E^2\phi^2} \qquad (5)$$

Stage III

$$M = \int_{A_f} \sigma dAy + \int_{y_o}^{c_t} \sigma_{yw} t_w dy \cdot y + \int_{y_o}^{c_b} \sigma_{yw} t_w dy \cdot y + 2\int_{0}^{y_o} \sigma t_w dy \cdot y$$

$$= E\phi(I_{ft} + I_{fb}) + \sigma_{yw} t_w \left(\frac{c_t^2}{2} - \frac{y_o^2}{2}\right) + \sigma_{yw} t_w \left(\frac{c_b^2}{2} - \frac{y_o^2}{2}\right) + 2\sigma_{yw} \frac{t_w y_o^2}{3}$$

$$M = E\phi(I_{ft} + I_{fb}) + \sigma_{yw}\left(\frac{t_w c_t^2}{2} + \frac{t_w c_b^2}{2}\right) - \sigma_{yw} \frac{t_w y_o^2}{3}$$

where $$Z_w = \left(\frac{t_w c_t^2}{2} + \frac{t_w c_b^2}{2}\right)$$

and $$y_o = \frac{\sigma_{yw}}{E\phi}$$

Therefore

$$M = E\phi\,(I_{ft} + I_{fb}) + \sigma_{yw} Z_w - \frac{t_w \sigma_{yw}^3}{3E^2\phi^2} \qquad (8)$$

Stage IV

$$M = \int_{c_t}^{d_t} \sigma_{y_3} b_t dy \cdot y + \int_{A_{fb}} \sigma dAy + \int_{y_o}^{c_t} \sigma_{yw} t_w dy \cdot y + \int_{y_o}^{c_b} \sigma_{yw} t_w dy \cdot y + 2\int_{0}^{y_o} \sigma t_w dy \cdot y$$

$$= \sigma_{y_3} b_t \left(\frac{d_t^2}{2} - \frac{c_t^2}{2}\right) + E\phi I_{fb} + \sigma_{yw} Z_w - \frac{t_w \sigma_{yw}^3}{3E^2\phi^2}$$

where $$Z_{ft} = b_t\left(\frac{d_t^2}{2} - \frac{c_t^2}{2}\right)$$

Therefore

$$M = \sigma_{y_3} Z_{ft} + E\phi I_{fb} + \sigma_{yw} Z_w - \frac{t_w \sigma_{yw}^3}{3E^2\phi^2} \tag{11}$$

Stage VI

$$M = \int_{c_t}^{d_t} \sigma_{y_3} b_t dy \cdot y + \int_{c_b}^{d_b} \sigma_{y_4} b_b dy \cdot y + \int_{y_o}^{c_b} \sigma_{yw} t_w dy \cdot y + \int_{y_o}^{c_t} \sigma_{yw} t_w dy \cdot y$$

$$+ 2 \int_{0}^{y_o} \sigma t_w dy \cdot y$$

$$= \sigma_{y_3} b_t \left(\frac{d_t^2}{2} - \frac{c_t^2}{2}\right) + \sigma_{y_4} b_b \left(\frac{d_b^2}{2} - \frac{c_b^2}{2}\right) + \sigma_{yw} Z_w - \frac{t_w \sigma_{yw}^3}{3E^2\phi^2}$$

$$M = \sigma_{y_3} Z_{ft} + \sigma_{y_4} Z_{fb} + \sigma_{yw} Z_w - \frac{t_w \sigma_{yw}^3}{3E^2\phi^2} \tag{14}$$

For sections which only have symmetry about an axis in the plane of bending, the position of the neutral axis at any stage of loading must be such that equilibrium of horizontal forces is maintained. Thus, the neutral axis of a tri-plate beam actually shifts as the stresses on the beam are increased. However, because of the particular nature of the tri-plate beam cross section used in this study, this shifting of the neutral axis was determined to be very small. It was assumed that such a minimal movement of the neutral axis would not appreciably influence the theoretical calculations. For the purpose of this study, the theoretical analysis is thus based on a stationary neutral axis.

APPENDIX B

DERIVATION OF THEORETICAL DEFLECTION EQUATION

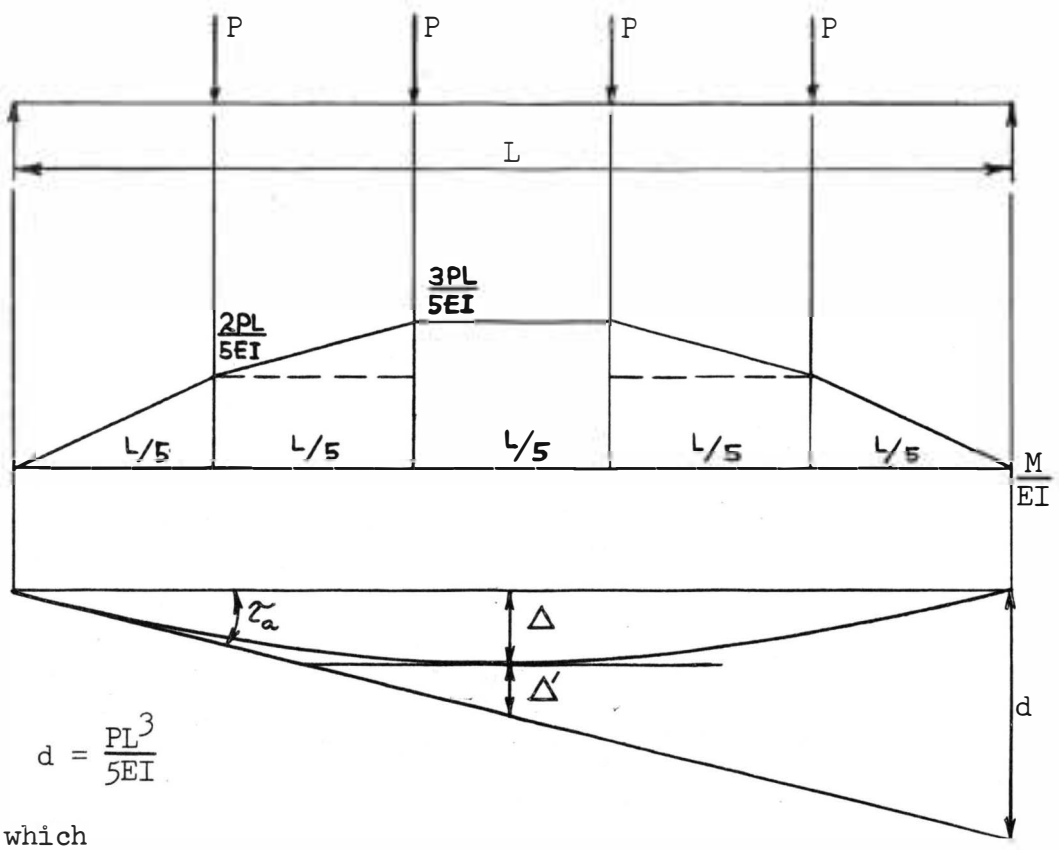

$$d = \frac{PL^3}{5EI}$$

From which

$$\tau_a = \frac{d}{19} = \frac{PL^3}{95EI}$$

$$\Delta = \frac{19}{2}\tau_a - \Delta'$$

and

$$\Delta' = \frac{111PL^3}{3000EI}$$

Therefore

$$\Delta = \frac{19}{2}\ \frac{PL^3}{95EI} - \frac{111PL^3}{3000EI}$$

$$\Delta = \frac{63PL^3}{EI} \times 10^{-3} \qquad (20)$$

APPENDIX C

PUMP LOAD, ACTUAL LOAD, AND ACTUAL MOMENT RELATIONSHIP FOR EACH SPECIMEN

Pump Readings, Actual Load, and Actual Moment Relationship

Dial Readings	Beam HS-2		Beam TS-3		Beam TS-4	
	W lbs	M ft-lbs	W lbs	M ft-lbs	W lbs	M ft-lbs
0	1,100	3,135	1,000	2,850	1,000	2,850
2	3,380	9,633	3,280	9,348	3,280	9,348
4	5,660	16,131	5,560	15,846	5,560	15,846
6	7,940	22,629	7,840	22,344	7,840	22,344
8	10,220	29,127	10,120	28,842	10,120	28,842
10	12,500	35,625	12,400	35,340	12,400	35,340
12	14,780	42,123	14,680	41,838	14,680	41,838
14	17,060	48,621	16,960	48,336	16,960	48,336
16	19,340	55,119	19,240	54,834	19,240	54,834
18	21,620	61,617	21,520	61,332	21,520	61,332
20	23,900	68,115	23,800	67,830	23,800	67,830
22	26,180	74,613	26,080	74,328	26,080	74,328
24	28,460	81,111	28,360	80,826	28,360	80,826
26	30,740	87,609	30,640	87,324	30,640	87,324
28	33,020	94,107	32,920	93,822	32,920	93,822
30	35,300	100,605	35,200	100,320	35,200	100,320
32	37,580	107,103	37,480	106,818	37,480	106,818
34	39,860	113,601	39,760	113,316	39,760	113,316
36	42,140	120,099	42,040	119,814	42,040	119,814
38	44,420	126,597	44,320	126,312	44,320	126,312
40	46,700	133,095	46,600	132,810	46,600	132,810